Title

Galactic cosmic ray simulation at the NASA space radiation laboratory — Progress, challenges and recommendations on mixed-field effects

Authors

Huff, Janice L

Poignant, Floriane

Rahmanian, Shirin

et al.

Publication Date

2023-02-01

DOI

10.1016/j.lssr.2022.09.001

Life Sciences in Space Research 36 (2023) 90–104

Contents lists available at ScienceDirect

Life Sciences in Space Research

journal homepage: www.elsevier.com/locate/lssr

Review article

Galactic cosmic ray simulation at the NASA space radiation laboratory – Progress, challenges and recommendations on mixed-field effects

Janice L. Huff [a,*], Floriane Poignant [b], Shirin Rahmanian [b], Nafisah Khan [b], Eleanor A. Blakely [c], Richard A. Britten [d], Polly Chang [e], Albert J. Fornace [f], Megumi Hada [g], Amy Kronenberg [c], Ryan B. Norman [a], Zarana S. Patel [h,i,1], Jerry W. Shay [j], Michael M. Weil [k], Lisa C. Simonsen [l], Tony C. Slaba [a]

[a] NASA Langley Research Center, Hampton, VA, 23681, United States of America
[b] National Institute of Aerospace, Hampton, VA, 23666, United States of America
[c] Lawrence Berkeley National Laboratory, Berkeley, CA, 94720, United States of America
[d] Department of Radiation Oncology, Department of Microbiology and Molecular Cell Biology, Leroy T Canoles Jr. Cancer Center, School of Medicine, Eastern Virginia Medical School, Norfolk, VA, 23507, United States of America
[e] SRI International, Menlo Park, CA, 94025, United States of America
[f] Georgetown University, Washington, DC, 20057, United States of America
[g] Prairie View A&M University, Prairie View, TX, 77446, United States of America
[h] KBR Inc., Houston, TX, 77058, United States of America
[i] NASA Johnson Space Center, Houston, TX, 77058, United States of America
[j] University of Texas Southwestern Medical Center, Dallas, TX, 75390, United States of America
[k] Colorado State University, Fort Collins, CO, 80523, United States of America
[l] NASA Headquarters, Washington, DC, 20546, United States of America

ARTICLE INFO

Keywords:
Space explorer
Space radiation
Galactic cosmic rays
Cancer risk
Central nervous system risk
Radiobiology

ABSTRACT

For missions beyond low Earth orbit to the moon or Mars, space explorers will encounter a complex radiation field composed of various ion species with a broad range of energies. Such missions pose significant radiation protection challenges that need to be solved in order to minimize exposures and associated health risks. An innovative galactic cosmic ray simulator (GCRsim) was recently developed at the NASA Space Radiation Laboratory (NSRL) at Brookhaven National Laboratory (BNL). The GCRsim technology is intended to represent major components of the space radiation environment in a ground analog laboratory setting where it can be used to improve understanding of biological risks and serve as a testbed for countermeasure development and validation. The current GCRsim consists of 33 energetic ion beams that collectively simulate the primary and secondary GCR field encountered by humans in space over the broad range of particle types, energies, and linear energy transfer (LET) of interest to health effects. A virtual workshop was held in December 2020 to assess the status of the NASA baseline GCRsim. Workshop attendees examined various aspects of simulator design, with a particular emphasis on beam selection strategies. Experimental results, modeling approaches, areas of consensus, and questions of concern were also discussed in detail. This report includes a summary of the GCRsim workshop and a description of the current status of the GCRsim. This information is important for future advancements and applications in space radiobiology.

Abbreviations
ARMIT, Associative Recognition Memory and Interference Touchscreen;
BFO, blood-forming organ;
BNL, Brookhaven National Laboratory;

* Corresponding author at: 2 West Reid Street, NASA Langley Research Center, Hampton, VA, 23681-2199.
E-mail address: janice.l.huff@nasa.gov (J.L. Huff).

[1] This work was prepared while Z.S. Patel was employed at KBR/NASA JSC. The opinions expressed in this work are the author's own and do not reflect the view of the National Institutes of Health, the Department of Health and Human Services, or the United States government.

https://doi.org/10.1016/j.lssr.2022.09.001
Received 22 May 2022; Received in revised form 1 September 2022; Accepted 5 September 2022
Available online 10 September 2022

CA, chromosome aberration;
CNS, central nervous system;
CVD, cardiovascular disease;
GCR, galactic cosmic radiation;
GCRsim, galactic cosmic ray simulator;
GI, gastro-intestinal;
Geant4, Geometry And Tracking;
Gy, Gray;
HIMAC, heavy ion medical accelerator in Chiba;
HZE, high charge and high energy ions;
IEA, incremental effects additivity;
LET, linear energy transfer;
MCM, medical countermeasure;
MSM, multiscale modeling;
NSNA, neither-synergy-nor-antagonism;
NSRL, NASA Space Radiation Laboratory;
RBE, relative biological effectiveness;
RER, relative effects ratio;
RITCARD, radiation-induced tracks, chromosome aberration, repair and damage;
RITRACKS, relativistic ion tracks;
Sv, Sievert;
vs., versus

1. Introduction

Characterizing in-flight and long-term health consequences for missions planned within Artemis (https://www.nasa.gov/what-is-artemis) will require extrapolating beyond our relatively limited spaceflight experience base, thereby introducing significant uncertainty and additional risk. For space radiation exposure, there are multiple adverse health effects that need to be characterized, which include carcinogenesis, central nervous system (CNS) decrements, and cardiovascular disease (CVD) (https://humanresearchroadmap.nasa.gov/evidence).

Models have been developed to calculate various risk metrics for space radiation induced cancer and are used operationally at NASA. These models are centered on disease risk estimates from human terrestrial radiation epidemiology (NRC 2006; UNSCEAR 2008; Preston 2007; Little 2008); however, significant uncertainties and knowledge-gaps remain (Cucinotta 2013a,2021). Uncertainty in the NASA cancer risk model is currently estimated to be a fold-factor of ~3.6 (equivalent to a relative uncertainty of 260%).[2] In that regard, equally plausible and widely available models for projecting space radiation induced cancer mortality were recently considered within an ensemble framework (Simonsen 2021). For mission exposures relevant to the Artemis program, individual models within the ensemble yielded mean cancer risk projections that differed by a factor of two or more. Such results suggest that even central estimates of risk, which should be anchored to the bulk of available epidemiological and radiobiological data, exhibit large uncertainties beyond what is characterized within the NASA model alone.[3]

A preliminary model for quantifying CVD mortality risk was developed (Cucinotta 2013b) based on similar scaling concepts as the NASA cancer risk model. Limited experimental data in rodent systems provide some insight into possible risks for CNS decrements as well (Liu 2019; Kiffer 2019; Cucinotta 2019; NCRP 2019), but insufficient human epidemiological data exist to serve as a basis for risk estimation for exposure levels of concern for spaceflight. In both cases however, there is at least some indication that these risks could be commensurate with radiation induced cancer mortality risk for crewmembers. The uncertainties in such projections are necessarily larger than those associated with cancer mortality given the comparatively small amount of data and the limited mechanistic understanding associated with either of these non-cancer endpoints.

As part of a strategy to reduce the large uncertainties associated with the biological effects of particle radiation, experiments are conducted at ground-based accelerator facilities using small animals or cell culture models. Primarily due to facility constraints, early experiments utilized beams comprising a single particle type and energy (e.g., 1 GeV/n ^{56}Fe). Viewed individually, these single-beam experiments provide an incomplete analog of the complex space radiation environment. Viewed collectively, however, the experimental data sets obtained from single-beam experiments cover a broad range of particle types and energies of direct relevance to space radiation protection and crew health. These data form the basis of scaling factors used in health risk assessment models and have led to important mechanistic understanding and the development of predictive computational models. Nonetheless, improved ground-based experimental analogs are still needed to further reduce risk projection uncertainties and validate predictive models, as well as to enable countermeasure development and testing in a relevant space environment.

It is within this context that the GCR simulator (GCRsim) at the NASA Space Radiation Laboratory (NSRL) was developed. The NSRL GCRsim is intended to deliver the deep space, shielded tissue radiation field to relevant biological targets in a laboratory setting. Preliminary design considerations of the GCRsim were studied by Slaba (2016) and focused mainly on the reference field specification and beam selection strategies. The term reference field refers to the space radiation environment being simulated. In defining the reference field, a broad range of mission architectures, shielding configurations, and physical quantities were considered. It was found that tissue doses (Gy), tissue dose equivalents (Sv), and spectral quantities such as flux as a function of linear energy transfer (LET), exhibited minimal variation within regions of interest to human risk. Solar activity effects were assessed, and it was determined that the main difference between solar minimum and solar maximum is the exposure-rate, while spectral characteristics of the radiation field encountered by humans in space behind shielding remain qualitatively similar between these two extremes. A single reference field for GCRsim development was ultimately identified as the radiation environment found within the blood-forming organ (BFO) of a human behind 20 g/cm^2 of aluminum shielding during solar minimum. It was shown that results for this organ and shielding level adequately represented the highly diverse shielding configurations analyzed. The BFO sites are also distributed throughout the body and therefore naturally provide a useful body-averaged surrogate.

Slaba (2016) next examined the impact of facility constraints on preliminary GCRsim design considerations. The NSRL can deliver protons up to 4 GeV and heavier ions up to 1.5 GeV/n. It was shown that approximately half of the exposure behind simple shielding configurations is lost if the energies above approximately 1.5 GeV/n cannot be represented in the external field. Conversely, ~90% of the shielded, local tissue environment (i.e., the collection of primary and secondary particles found within human body tissues) can be represented within current facility capabilities with energies of protons up to 2.5 GeV, helium up to 1.5 GeV/n, and heavier ions up to 1.5 GeV/n. This distinction between the external field impinging on the vehicle or habitat shielding and the local field found within radiosensitive tissues, illustrated in Fig. 1, is an important aspect of GCRsim design and is discussed later in this paper. Suffice to note here that the NSRL GCRsim is based on the local field approach, Fig. 1B, wherein a discrete set of beams are chosen to directly represent the reference field, and no shielding or moderator blocks are placed in the beam line. Finally, a systematic method for beam selection within this design concept was defined, and it was shown that a practical number of beams accurately reproduced the dose, dose equivalent, and spectral fluence quantities defined for the reference field

[2] The fold-factor is calculated as the ratio of the upper 95% confidence interval bound risk to the median risk.

[3] The NASA cancer risk model propagates parameter uncertainties into risk assessments using Monte Carlo methods. Uncertainties associated with underlying model assumptions, or model-form, are not explicitly characterized.

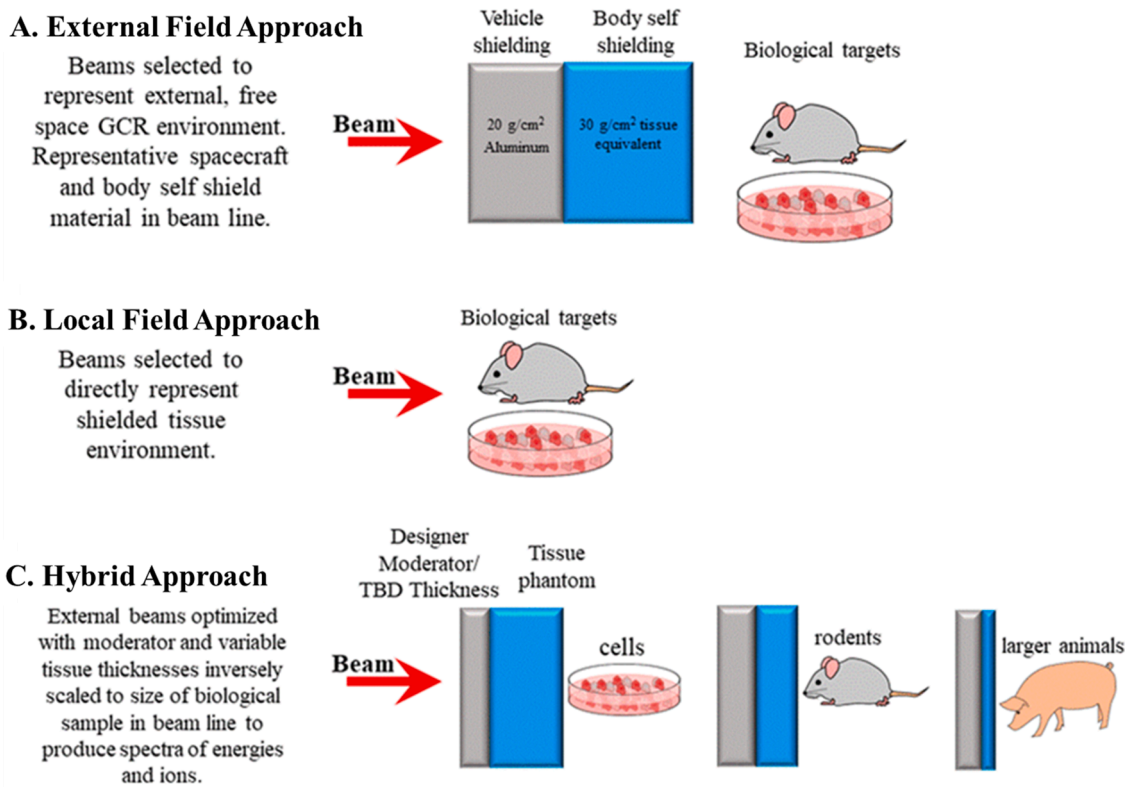

Fig. 1. General approaches for ground-based GCRsim. Panel A illustrates the external field approach, where a combination of beams and shielding are chosen such that the radiation field impinging on biological targets closely represents the reference field. Panel B shows the local field approach, where beams are chosen directly to represent the reference environment. Panel C illustrates the hybrid approach based on optimization of the external and local field approaches requiring further research (Simonsen 2020).

(Slaba 2016).

Results from this initial study were presented at the NASA Human Research Program Investigators' workshop in 2015 (Slaba 2015) and discussed at length by attendees. Discussion continued beyond the workshop and was expanded to include international research partners, ultimately leading to the opinion paper of Norbury and over 40 co-authors (Norbury 2016). A broad range of topics pertaining to GCRsim design were addressed in the paper. It was concluded that the local field approach was most appropriate for a baseline GCRsim capability at NSRL given the known energy constraints. It was also recommended that further work should be done to optimize simulator design while retaining connections to the single-beam experimental data

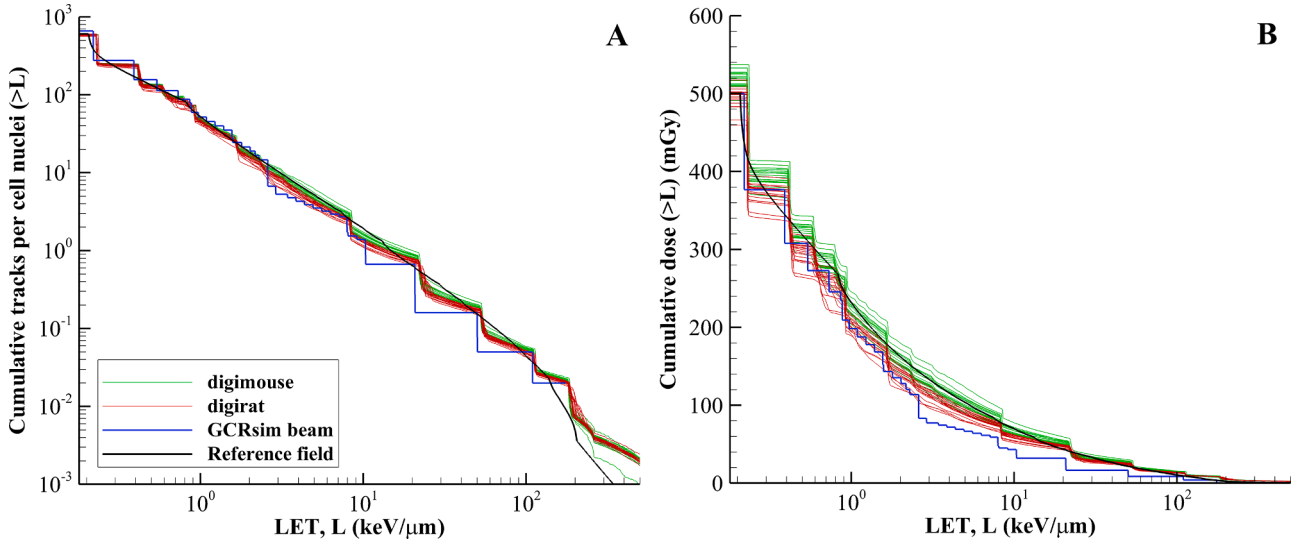

Fig. 2. Comparison of reference field to the GCRsim beam and corresponding simulated spectra obtained inside mouse (Digimouse – a 3D mouse atlas from http://neuroimage.usc.edu/neuro/Digimouse) and rat (Digirat – a scaled version of Digimouse) phantoms. Panel A shows the fluence spectra in terms of tracks per cell nuclei (100 μm^2). Panel B shows the dose spectra (mGy). Both results are normalized to a total dose of 500 mGy, which is within the range of exposure estimates for a long duration Mars mission (Valinia 2022) and can be directly scaled to any other desired dose. Multiple green and red lines correspond to results for various tissues in the phantoms. Details of the simulation approach can be found in (Simonsen 2020). To view figure in color, access the online version.

collected previously.

The first NSRL GCRsim was defined in 2017 (Simonsen 2020). Given the incomplete information on mixed-field radiation effects available at the time, the definition was guided by optimizing across reference field quantities, NSRL facility constraints, animal care and cellular model requirements, and the desire to maximize overlap with historical single beam data. The GCRsim beam includes 33 mono-energetic beams covering the particles, energies, and LET of interest to human health. A comparison between the reference field and GCRsim beam is shown in Fig. 2, along with the simulated spectra obtained at various tissues inside mouse and rat phantoms. The purpose of such a comparison is to demonstrate that the GCRsim beam and corresponding simulated spectra inside commonly used experimental systems (mice and rats) agree well with the reference environment over the full range of LET. Details of the simulation results can be found in Simonsen (2020). The simulated fluence and dose spectra inside the phantoms agree well with the reference field across the full range of LET.

Beam ordering, concept-of-operations, and contingency plans were defined to support acute exposures and fractionated exposures carried out over multiple weeks. NSRL can reliably deliver the 33 beams sequentially in approximately 75 min. A simplified GCRsim using 5-ions was also defined, which requires less time for set-up and delivery while remaining compatible/consistent with the full GCRsim. Discussion of beam delivery times and possible overlap with certain biological response and repair time scales is provided in Section 4.

There have been several experiments using the full GCRsim, the simplified GCRsim, and other mixed-field definitions, especially over the past five years. The data and experiences collectively gained from these efforts provided the opportunity to evaluate the suitability of the NSRL GCRsim for its stated purpose. A GCRsim workshop was held virtually in December 2020. Workshop attendees included principal investigators of NASA-funded studies, NASA scientists, NASA managers and staff scientists from the NSRL. The workshop included a full day of scientific presentations followed by a half day of discussion with the goal of answering the following questions:

- Is there any experimental evidence suggesting that simplifications, modifications, or improvements to the GCRsim beam are needed?
- What future studies need to be performed to improve the GCRsim mixed-field definition?
- Does the current GCRsim beam adequately represent the radiation environment that will be encountered by humans in deep space behind shielding?

It was recognized that the concepts of mixed-field and dose-rate effects may be intrinsically coupled. Nevertheless, discussions within the workshop remained largely focused on the NSRL GCRsim mixed-field definition.

In this paper, we provide a summary of the workshop findings, observations, and recommendations related to the NSRL mixed-field definition. In Section 2 an overview of the current NASA GCRsim format is given, which includes a description of the beam characteristics and a comparative discussion of alternative GCRsim design approaches. In Section 3, experimental and modeling efforts focused on mixed-field effects that were presented at the workshop are summarized. Workshop discussion topics are broadly organized in Section 4 into three main areas: areas of consensus (4.1), contradictory results or evidence (4.2), and open questions (4.3).

2. Brief overview of the current GCR simulator at NASA

2.1. NSRL GCRsim beam

The NSRL GCRsim beam parameters are summarized in Table 1. The beam encompasses ions with charge (Z) between $Z = 1$ and $Z = 26$, energies between 20 MeV/n and 1000 MeV/n, LET between 0.2 keV/μm and 175 keV/μm, and can be delivered in approximately 75 min. In the case of the ^{1}H and ^{4}He beams, a polyethylene degrader system is used to generate a pseudo-continuous low energy spectrum. The 100 MeV/n beam for both particle species is degraded into 10 distinct energies with a lower limit of 20 MeV/n. Further discussion and rationale for the binning structure is provided by Simonsen (2020). It is important to point out though that Z = 1, 2 ions with energy below 100 MeV/n account for ~36% of the dose in radiosensitive organs. Extra fidelity for this ion/energy region is needed to simultaneously reproduce the dose and fluence spectrum of the reference environment while maintaining reasonably homogeneous dose profiles within rodent systems.

Table 1
NSRL GCRsim beam parameters normalized for a total dose of 500 mGy, which is within the range of exposure estimates for a long duration Mars mission (Valinia 2022). Values can also be directly scaled to any other desired dose.

	Energy (MeV/n)	LET (keV/μm)	Range (cm)	Dose (mGy)	Tracks per 100 μm^2 cell nucleus
^{1}H	20–100	0.7 – 2.6	0.4 – 7.8	140.6	71.6
	150	0.5	15.9	35.0	40.2
	250	0.4	38.1	68.9	110.4
	1000	0.2	326.6	123.6	349.6
^{4}He	20–100	2.9 - 10.3	0.4 – 7.8	39.6	4.7
	150	2.2	16.0	7.5	2.1
	250	1.6	38.3	16.4	6.6
	1000	0.9	327.8	24.9	17.6
^{12}C	1000	7.8	110.1	11.7	0.9
^{16}O	350	20.8	17.0	15.4	0.5
^{28}Si	600	50.2	22.7	8.1	0.1
^{48}Ti	1000	109.5	32.5	4.5	0.03
^{56}Fe	600	175.1	13.1	4.1	0.01

Numerous radiobiology experiments suggest that the ordering of ion exposures can influence observed biological responses, and this effect was explicitly discussed in the workshop. The GCR environment may be generally thought of as a continuous shower of protons with interspersed helium and sporadic heavy ions. The ordering of ion delivery in the GCR simulator is therefore defined to approximate this behavior to the extent possible. Protons and helium are frequently delivered (majority of the dose is delivered first and last in the sequence) with sporadic heavy ions throughout the sequence.

NASA has also defined a simplified GCRsim (Simonsen 2020), composed of only six ion beams (five different ions with protons at two different energies), which can be delivered in 20 min (Table 2). The simplified GCRsim beam was defined for collection of preliminary data, countermeasure screening studies and initial understanding of mixed-field effects (Simonsen 2020). The beam order and dose fractions used in the simplified GCRsim are consistent with the full GCRsim, with protons constituting most of the exposure and delivered first and last in the sequence. While spectral characteristics of the reference field are not as accurately captured by the simplified GCRsim, the selected beams still provide uniform dose profiles in both mice and rat models (Simonsen 2020). The complexity of the GCR simulator, including how many beams are sufficient, and whether the 6 ion beams are adequate, was a topic covered in this workshop, and will be discussed in later sections.

The beams are delivered by the GCR simulator in the following order (ion beam followed by their energy in MeV/n):

Table 2
Beam definition for the simplified 5-ion GCRsim.

	Energy (MeV/n)	Dose contribution (%)	Delivery order
^{1}H	1000	35	1
^{28}Si	600	1	2
^{4}He	250	18	3
^{16}O	350	6	4
^{56}Fe	600	1	5
^{1}H	250	39	6

- (^{1}H 1000), (^{4}He 1000), (^{28}Si 600)
- (^{1}H 20), (^{1}H 23), (^{4}He 20), (^{4}He 23), (^{48}Ti 1000)
- (^{4}He 27), (^{4}He 32), (^{1}H 27), (^{1}H 32) (^{1}H 37), (^{1}H 43), (^{4}He 37), (^{4}He 43), (^{16}O 350)
- (^{4}He 50), (^{4}He 58), (^{1}H 50), (^{1}H 58) (^{1}H 68), (^{1}H 80), (^{4}He 68), (^{4}He 80), (^{12}C 1000)
- (^{4}He 100), (^{1}H 100), (^{1}H 150), (^{4}He 150), (^{56}Fe 600)
- (^{4}He 250), (^{1}H 250)

2.2. Other approaches

The NSRL GCRsim is based on the local field approach described briefly in Section 1 and illustrated in Fig. 1B. For this concept, models are used to characterize the radiation field found within radiosensitive tissues – the reference field. A set of mono-energetic ion beams is used to collectively represent the particles and energies found in the reference field, as shown in Table 1.

The external field approach, illustrated in Fig. 1A, manifests a very different set of requirements and practical considerations compared to the local field approach. For this concept, a moderating shield is placed within the beam line and irradiated with one or more mono-energetic ions; the biological target or sample is placed downstream of the moderator, although not necessarily along the main beamline. As the energetic primary ion beam interacts with the shield, nuclear collisions yield a spectrum of secondary particles produced over a broad range of energies and angles. The primary ion beam may be stopped by the shield or allowed to penetrate through and reach the intended target(s) depending on the design parameters.

There have been variations of the external field approach published over the past few years. Kim (2015) developed a simulator concept requiring nine heavy ion ($Z > 2$) beams and at least 10 distinct energetic beams for protons and helium. Unique absorber thicknesses were prescribed for each of the beams to broaden the energy distributions of primary and secondary particles. The approach was shown to produce a radiation field that adequately represents the space environment in terms of charge and energy-segregated dose.

Timoshenko (2017) proposed an idea based on using 12 GeV protons with multiple absorbers placed at distinct locations along the beam line. Biological targets are placed off-axis from the beam to capture a superposition of secondary nucleons produced in each of the absorbers at different angles. The method yields continuous nucleon spectra that were qualitatively compared to simulations of the space environment. In a companion study, (Gordeev 2021), considered a 1 GeV/n ^{56}Fe beam incident on an axially rotating cylindrical absorber. The cylinder is constructed by sets of circular targets that each cover only partial sectors of the full circular cross section. Simulation results showed that this approach can produce heavy ions with broad energy distributions.

Chancellor (2017) used a 1 GeV/n ^{56}Fe beam with a complex moderator block placed along the beam line. Details of the block were not provided; however, a complex geometric volume comprising multiple materials is alluded to in the report. Simulation results were compared to spaceflight LET spectra and showed reasonable agreement above 10 keV/μm.

Schuy (2020) used a design with fast energy switching of 400 MeV/n, 700 MeV/n, and 1 GeV/n ^{56}Fe beams incident on detailed periodic absorbers specifically designed for each of the energies. Proposed methods for designing and optimizing the absorbers were described, but no verification or simulation results were provided for GCR in the initial study.

Although not discussed at the workshop, it should be noted that other irradiation facilities are being developed and utilized to study aspects of the high LET component of the space environment and to evaluate combined effects of radiation and simulated microgravity. Takahashi (2020) developed the Simulator of the environments on the Moon and Mars with Neutron irradiation and Gravity (SwiNG) to study the combined effects of high LET irradiations and microgravity conditions. Borak et al. (2019) developed a combined neutron/gamma irradiator allowing both acute and prolonged chronic exposures to be developed to help assess dose-rate effects for high LET irradiations. These facilities provide useful information for targeted components of the space environment. Likewise, simulation of microgravity at the NSRL and how this may modify radiation responses were not topics of discussion at this workshop but could be addressed in the future.

There is notable diversity in the implementation features of these external field approaches due, in some cases, to the diverse constraints associated with the different facilities. Some concepts were not necessarily optimized for a specific facility. The number of beams used, beam types, and beam energies all vary, as do the number and placement of absorbers along the beamline, geometry, and materials used. Nonetheless, there are primary distinctions that can be drawn between these approaches relative to the NSRL GCRsim. The presence of shielding in the beamline produces a true mixed field of primary and secondary ions and neutrons incident on a biological sample, which is different than the NSRL GCRsim that achieves an accumulated mixed field in ~75 min through a rapid sequence of mono-energetic, single-ion beams. Neutrons are not explicitly included in the NSRL GCRsim beam; although, it is important to recognize that dominant aspects of neutron dose (proton recoils and inelastic reaction products with $Z \leq 2$) are included in the charged particle beams (Simonsen 2020). More details on the neutron dose components included in the NSRL GCRsim are provided in Section 4.

Dosimetry requirements to fully characterize the NSRL GCRsim were quite minimal since only a time-accumulated characterization of individual beams was needed, which was easily accomplished with the existing dosimetry system used for single beam studies for many years. Though none of the external field approaches have reached operational status yet, dosimetry requirements in mixed GCR beams may be substantial and cannot be ignored in design studies. Characterization of the beam emerging from one or more moderator blocks must include discrimination of particle charge and energy over the ranges of interest to multiple human risks. Simple measurements of absorbed dose or LET spectra behind the moderator block(s) will be insufficient to enable complete interpretation of experimental results. These topics, along with the impact of secondary neutrons, were discussed at length by workshop attendees. A summary of the discussion is provided in Section 4.1.2.

3. Experimental data and computational models to evaluate mixed-field effects

As stated in Section 1, there have been several studies utilizing the simplified GCRsim beam, full GCRsim beam, and other mixed-ion exposure regimens over the past ~five years. Per design, many of these were able to make use of historical single-ion datasets to test specific hypotheses related to mixed-field biological responses. Importantly, these early GCRsim studies offer an opportunity to shed light on the adequacy of the NSRL GCRsim mixed-field definition. Important advancements in predictive model capabilities have also been made and are critical for continued progress. This section summarizes recent experimental and modeling progress pertaining to mixed-field effects in the context of the NSRL GCRsim.

3.1. Predictive computational modeling

Significant progress has been made in recent years to help interpret and translate between single-ion and GCRsim experimental results. In combination with experimental data, these computational models also have the potential to improve the characterization of radiation quality effects and advance human health risk assessment. This section summarizes computational models developed or improved upon to describe mixed-field effects of interest to GCRsim.

Ham (2017); Huang (2019, 2020) developed an incremental effect additivity model to predict experimental dose-response relationships for

mixed-ion exposures. The model assumes such predictions can be made if the corresponding dose-responses for the single-beams comprising the mixed-ion composition are known *a priori*. Different dose-response relationship models, including targeted and non-targeted effects, can be tested within the theoretical and computational framework. Important to their work is the evaluation of 95% confidence intervals, accounting for the correlation between the adjustable parameters. Comparison of these intervals from the different models to experimental data enables statistical tests for synergy (i.e., combination of multiple beams yields a response that exceeds incremental effect additivity and exceeds Loewe additivity) or antagonism (i.e., combination of multiple beams is sub-additive) (Loewe 1926, 1928; Azasi 2020; Lederer 2019). In principle, the incremental effect additivity approach can be applied to any endpoint and therefore offers a means of evaluating beam complexity requirements in the NSRL GCRsim as data become available. This modeling approach may also become particularly important in the context of cancer risk assessment models, where simple additivity in mixed-field exposures is still assumed (Cucinotta et al. 2013a; Simonsen 2021).

Slaba (2020) developed an integrated, multi-scale model (MSM) utilizing Geant4 (Agostinelli 2003), RITRACKS (Plante 2019a), and RITCARD (Plante 2019a) to predict chromosome aberrations (CA) in cells exposed to either sequential mixed beams or complex radiation fields produced by beam interactions with shielding. Briefly, for a given experimental setup, Geant4 is used to describe the beam interactions with shielding and/or the biological sample of interest. Relevant mass along the beamline, including air, measurement devices, and sample holders can be included in the simulation, along with the NSRL target room. The simulated fluence of particles impinging on the biological sample of interest is used as input to the track-structure simulation code, RITRACKS, to describe energy deposition characteristics at the nanometer scale. This information is then provided to RITCARD to describe the cellular damage and repair processes leading to CA formation. Damage classification and repair kinetics models in RITCARD have been greatly improved over the past few years (Plante 2019b), and simulation results are being benchmarked against experimental data for lymphocytes and fibroblasts to assess and improve predictions across several cell lines and over a large LET range. The MSM was used to predict experimental dose-response of human fibroblasts exposed to monoenergetic ion beams ^{1}H (344 MeV), ^{4}He (344 MeV/n), ^{16}O (450 MeV/n) or ^{56}Fe (950 MeV/n) behind 20 g/cm^2 of aluminum and 10.345 g/cm^2 of polyethylene, thus making a complex irradiation field. Predictions fell within the experiment error bars for most of the available data (Slaba 2020).

These predictive models offer multiple opportunities to improve radiation quality models used in cancer risk assessments. (Ham 2017; Huang 2019, 2020) have suggested that simple additivity may not be valid especially if non-linearities at low dose appear as a result of non-targeted effects. Aside from the obvious value of using the incremental effects additivity approach to predict and interpret mixed-ion experimental results, it may have greater value in providing an alternative to simple additivity used in risk assessment (or at least provide some measure of the uncertainty introduced by simple additivity in space applications). Similarly, the multi-scale simulation model has shown the ability to predict CA in a broad range of irradiation conditions including single-ions, sequential beams, and complex mixed fields (Slaba 2020). Continued validation is necessary, but the multi-scale simulation model provides a complimentary approach to incremental effects additivity that may also provide valuable surrogate information for quality factor models.

A conceptually distinct approach is to directly model the dose-response relationships obtained from GCRsim irradiation. In principle, such a model would give rise to a GCR relative biological effectiveness (RBE) factor or relative effects ratio (RER) (Shuryak 2017, 2021, 2022), circumventing the need for detailed quality factors defined over a broad range of particles and energies. The questions surrounding additivity of single particle responses for mixed fields are also avoided. The single RBE (or RER) value would be applied as a multiplicative factor to space relevant GCR doses (or risks) for use in risk assessment. Multiple questions surely arise in practical application of this approach; however, it bears noting in the broader discussion of modeling advancements relevant to ground-based analogs such as the GCRsim.

3.2. Cellular endpoints

3.2.1. Chromosome aberrations

Chromosome aberrations (CA) are a known consequence of exposure to ionizing radiation. Chromosome instability is one of the primary drivers for tumor initiation, thus making chromosome aberrations an endpoint of interest for carcinogenesis (Sridharan 2016). Previous studies on human cells have characterized radiation quality effects for mono-energetic ions with and without shielding (George 2003a, 2003b, 2007, 2013; Durante 2005), and studies are ongoing to assess the effect of mixed beams.

Hada (2021) compared CA (simple and total exchanges) for various related beam configurations and shielding. First, a 4-beam mixture comprising ^{1}H (344 MeV, 43.7%), ^{4}He (344 MeV/n, 18.9%), ^{16}O (450 MeV/n, 23.7%), and ^{56}Fe (950 MeV/n, 13.7%) was used to irradiate cells shielded by 20 g/cm^2 aluminum and 10 g/cm^2 polyethylene. The shield configuration allowed penetration of the ^{1}H and ^{4}He beams, but the primary ion energies were downshifted to ~250 MeV/n, on average. The heavier beams were fully stopped by shielding, allowing only secondary particles to reach the cells. The complex field produced by beam interactions in shielding was approximated using spectral binning procedures (Slaba 2016) by a 4-beam mixture comprising ^{1}H (250 MeV, 68.1%), ^{4}He (344 MeV/n, 20.3%), ^{16}O (350 MeV/n, 6.9%), and ^{48}Ti (300 MeV/n, 4.7%). Measured CA yields are statistically indistinguishable between the two scenarios (Hada 2021), providing support for the spectral binning approach used to guide NSRL GCRsim beam selection. Further analysis of these experimental data is ongoing, and comparisons with the MSM of Slaba (2020) will also be helpful, as it has already demonstrated the ability to predict CA for single ion and mixed-field configurations.

In another experiment, Hada (2021) investigated the effect of the beam order on the dose response for total exchanges. Human fibroblasts were irradiated at HIMAC, Japan using two beams, ^{1}H (150 MeV, 60%) and ^{12}C (290 MeV/n, 40%), with a 2 hr interval between beam switching. Preliminary results showed that the order of beam delivery may impact the dose response. Additionally, it was observed that irradiating cells with two beams appeared to result in more than an additive effect on the frequency of chromosome aberrations, thus suggesting some synergetic effect for this endpoint. Similar results were also observed in other 2-ion and 3-ion beam experiments with quick beam switching at NSRL for fibroblasts and lymphocytes, but not for epithelial cells (Hada 2021). However, experiments with a more complex 6-ion beam mixture appear to show less than additive effect on chromosome aberration total exchanges for human fibroblast. The extent of the effect depended on the dose.

3.2.2. Cell survival

Kronenberg et al. are investigating the effect of radiation on TK6 human lymphoblasts, which is a good model for sensitivity to ionizing radiation and for which there is substantial archival data from single ion exposures (Kronenberg 1989, 1995). Initial studies using a 3-ion beam comprising ^{1}H (250 MeV, 0.4 keV/μm, 70%), ^{20}Ne (353 MeV/n, 32 keV/μm, 15%) and ^{28}Si (383 MeV/n, 61 keV/μm, 15%), indicated it may be possible to predict the results for cell killing by considering a strictly additive model derived from individual ion beams (Kronenberg 2021). Results from ongoing studies address other genotoxic endpoints including mutation and consider other irradiation conditions focused on dose rate.

3.3. Animal endpoints

3.3.1. Harderian gland tumorigenesis

Historically, the largest tumor dataset available was obtained for harderian gland tumor prevalence for ion beams of LET varying from 0.4 keV/μm to 953 keV/μm (Alpen 1993; Alpen 1994; Chang 2016), thereby covering an important LET range of interest for space radiation protection. This database has provided important understanding for space radiation induced cancer risk and the dependence on particle type and energy. Recent efforts have thus converged towards obtaining the same endpoint but considering mixed beams. Analysis was performed with the incremental effects additivity approach to infer on possible synergy/antagonism.

Experimental tumor prevalence for 2-ion beams showed that one experimental approach, ^{1}H (250 MeV, 0.4 keV/μm) + ^{56}Fe (600 MeV/n, 193 keV/μm), 70 cGy, showed synergy (described in Section 3.1), while two others did not ^{28}Si (260 MeV/n, 70 keV/μm) + ^{56}Fe (600 MeV/n, 193 keV/μm), 40 cGy and ^{1}H (250 MeV, 0.4 keV/μm) + ^{28}Si (260 MeV/n, 70 keV/μm), 100 cGy (Huang 2020). Experimental and modeling results for the ^{1}H + ^{56}Fe case are shown in Fig. 3, where synergy was observed.

Additional experiments were conducted using a 3-ion beam of ^{28}Si (260 MeV/n, 70 keV/μm) + ^{48}Ti (1000 MeV/n, 100 keV/μm) + ^{56}Fe (600 MeV/n, 193 keV/μm) and for 2 doses (30 cGy and 60 cGy) delivered within 15 min, with doses evenly distributed between each ion (Blakely 2021). Separately, animals were either sham treated or exposed to a single 100 cGy dose of a 6-ion beam consisting of ^{1}H (250 MeV, 0.4 keV/μm) + ^{4}He (228 MeV/n, 1.6 keV/μm) + ^{16}O (350 MeV/n, 17 keV/μm) + ^{28}Si (260 MeV/n, 70 keV/μm) + ^{48}Ti (1000 MeV/n, 100 keV/μm) + ^{56}Fe (600 MeV/n, 190 keV/μm). Modeling of tumor prevalence for these mixed beam experiments was performed using the incremental effects additivity approach with targeted effects-only or targeted effects + non-targeted effects, and the results will be reported elsewhere.

3.3.2. Lung tumorigenesis and carcinogenesis

Previous studies on lung cancer were done to investigate the effect of both low and high-LET mono-energetic ion beams, with evidence showing an increased risk of lung tumor progression for high-LET beams (Asselin-Labat 2017; Luitel 2018). To better represent the space environment, Shay et al. investigated the effect of order of ion delivery of mixed ion beam on lung cancer progression using eight- to twelve-week-old male and female K-ras^{LA1} mice, evaluated at two time points (100 days and 1 year) (Luitel 2020). Several biological endpoints were measured, such as lipid peroxidation to characterize oxidative stress, and the number of premalignant lesions and invasive carcinomas. The authors used a 3-ion beam mixture composed of 20 cGy of ^{1}H (120 MeV, 0.64 keV/μm), 5 cGy of ^{4}He (250 MeV/n, 1.6 keV/μm) and 5 cGy of ^{28}Si (300 MeV/n, 70 keV/μm), which was delivered at a dose rate of 0.5 cGy/min. Two beam orders were considered, 3B-1 (^{1}H→^{4} He→ ^{28}Si) and 3B-2 (^{28}Si→ ^{4}He→ ^{1}H), both delivered in 66 min. Irradiation with a monoenergetic beam of 30 cGy ^{1}H (120 MeV) was included for comparison.

As shown in Fig. 4 from Luitel (2020), a significant increase of invasive lung adenocarcinomas was observed one-year post irradiation when protons were delivered first (3B-1), but not when Si ions were first (3B-2). Increased invasiveness was associated with an elevated level of oxidative stress and increased number of lesions at 100 days post irradiation. (Luitel 2020) also observed that when protons and helium were delivered first, and there was a 24 h interval before the Si ion exposure, that there was no increase in cancer incidence, which suggests that the order of the ion beam delivery matters during acute exposures, but that temporally spacing them out mitigates this effect (lowering the dose of silicon ions also attenuated this effect). Given the dose and LET of particles, it was estimated that every cell nucleus is traversed by ~150 protons, ~15 ^{4}He ions while only one in three cell nuclei is traversed by ^{28}Si ions. In the scenario where protons are delivered first (3B-1), all cells will contain damage, while for the scenario with Si ions delivered first (3B-2), only ~1 in 3 cells will contain damage at the end of the first irradiation. Thus, it is possible that during repair of initial damage there is a greater amount of open chromatin in the proton first scenario (3B-1), which might increase sensitivity to the formation of double strand breaks during the second and third exposures, thereby increasing carcinogenesis. Spacing out the irradiations allows time for DNA to fold back to a normal configuration following repair, thus attenuating the effect. While such a model could explain this effect, this might not be reflective of what occurs in deep space where the dose rate is much lower.

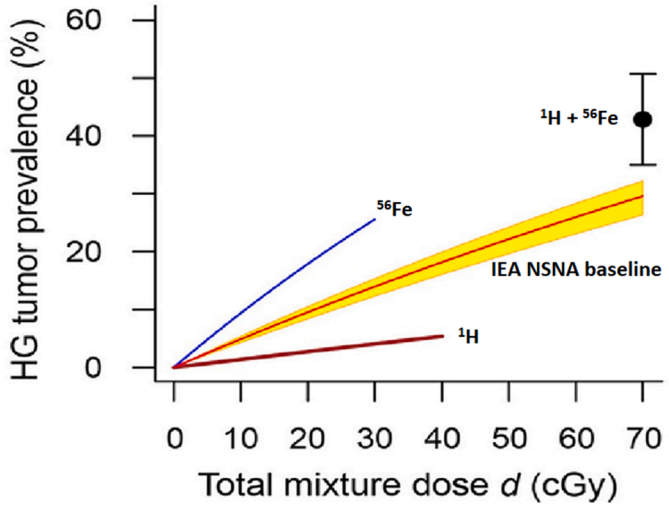

Fig. 3. Harderian gland (HG) tumor prevalence experimental data (black dot with error bar) and targeted-effects only model results for ^{1}H + ^{56}Fe exposure. The brown and blue curves are the ^{1}H and ^{56}Fe dose-effect models, respectively. The red curve is the incremental effects additivity neither-synergy-nor-antagonism (IEA NSNA) model result along with the 95% confidence level. (Huang 2020). To view figure in color, access the online version.

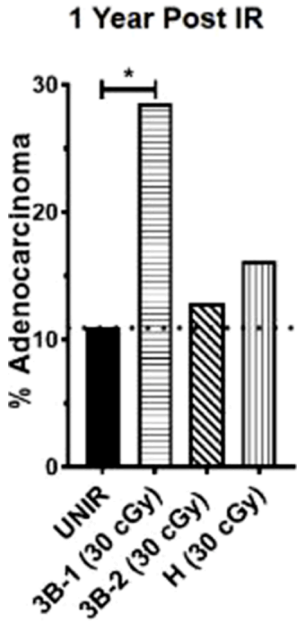

Fig. 4. Tumorigenic effect (lung) of multiple ion radiation in a K-ras^{LA-1} mouse model. Results are shown for unirradiated controls (UNIR), irradiation (IR) with a 30 cGy mixed beam ordered as ^{1}H →^{4}He→ ^{28}Si (3B-1) and ^{28}Si →^{4}He→ ^{1}H (3B-2), and irradiation with 30 cGy of ^{1}H (Luitel 2020).

Currently, this group is investigating the full GCRsim beam comparing acute (one hr) and chronic (four weeks) exposures to 50 cGy total dose. Similar data for 25 cGy and 75 cGy are under analysis. These data showed that, while after 100 days a persistent level of oxidative stress was observed, no significant increase in tumor initiation (100 days) was evident. Although a trend of increased invasive carcinoma (one year) was observed, it was not statistically significant.

3.3.3. Gastro-intestinal (GI) tumorigenesis

In previous work, Fornace at al. have shown a significantly higher risk of intestinal and colonic tumorigenesis for three mouse models of human colorectal cancer exposed to HZE as compared to γ-rays, even at low dose. In these studies, the mice were exposed to doses ranging from 5 cGy to 50 cGy and intestinal and colon tumor frequency and size were scored 150 days after exposure (Suman 2019; Kumar 2019). Recently, GI tumorigenesis was investigated 150 days post irradiation, for 6–8 week $APC^{1638N/+}$ male mice irradiated with 5 cGy single ions of ^{16}O (325 MeV/n, 22 keV/μm) or ^{28}Si (300 MeV/n, 69 keV/μm) vs. 50 cGy total dose of a 4-ion beam consisting of ^{1}H (1000 MeV, 1.26 keV/μm, 60%) + ^{4}He (250 MeV/n, 2 keV/μm, 20%) + ^{16}O (325 MeV/n, 22 keV/μm, 10%) + ^{28}Si (300 MeV/n, 69 keV/μm, 10%). Results to date indicate that the majority of the tumorigenesis can be ascribed to the HZE ions since an estimate of the additive results after single beam irradiation with ^{16}O plus ^{28}Si were comparable to that of the 4-ion beam (Fornace 2021). This study illustrates the importance of cross comparison of mixed field exposures with single ion studies.

3.3.4. Central nervous system and cognitive function

Alterations in cognitive and behavioral responses can be characterized by a variety of tests of varying complexity, including recognition memory, social memory, spatial memory, anxiety and attention (Cekanaviciute 2018). Basic tasks (e.g., novel object recognition) interrogate the functionality of defined brain regions and assess relatively simple cognitive processes, while complex cognitive tasks involve brain regions working in a highly complex manner, requiring neural network functioning in synchrony (e.g., creative problem solving, Associative Recognition Memory and Interference Touchscreen (ARMIT) task). Impairment of basic tasks would indicate extremely severe damage; however, mission success or failure will more likely depend upon the ability to perform complex cognitive tasks under pressure. In general, studies need to assess space-radiation induced CNS damages on multiple cognitive processes to have a complete assessment of the risks (Britten 2022).

As for other endpoints, until recently, the predominant strategy has been to assess the impact that exposure to single ions of defined energy/LET has on performance in a cognitive task. There is now a considerable body of evidence from ground-based rodent experiments to suggest that exposure to doses as low as 25 cGy of several ions (i.e. protons, ^{4}He ^{16}O, ^{28}Si, ^{48}Ti and ^{56}Fe) impairs various cognitive functions, including cognitive flexibility tasks (Acharya 2019; Britten 2014; 2018, 2020a, 2020b, 2022; Davis 2014; Hadley 2016; Jewell 2018; Parihar 2015, 2016, 2018; Burket 2021; Whoolery 2019; Soler 2021). The findings from these studies cover a relevant dose regime for sustained deep space habitat and Mars scenarios (Simonsen 2020). However, there is also a concern about whether the neurocognitive impairment data obtained from single ion studies will be representative of the severity, frequency or nature of cognitive deficits that arise following exposure to the GCR spectrum. The precise impacts on humans remain unknown at this time due to the lack of relevant epidemiological data from which risks may be estimated.

Currently, there are eight published studies on the impact of multi-ion exposure on cognitive performance (Britten 2022; Krukowski 2018a, 2021; Raber 2016, 2019, 2020, 2021; Schaeffer 2022). One study directly compared the impact of the simplified GCRsim with that of a single ion (^{4}He, 250 MeV/n) (Britten 2022). In that study, while exposure to 10 cGy simplified GCRsim adversely impacted problem-solving capabilities of female rats using the ARMIT task, exposure to 10 cGy ^{4}He did not. Whether this differential impact on cognitive performance is maintained in different cognitive tasks is currently unclear. Results from conference presentations suggest that GCRsim exposure impacts many other cognitive and psychosocial processes, but whether GCRsim is more detrimental than single ions, appears to be very context dependent, and may be neural network specific.

Two studies investigated exposure of female and male B6D2F1 mice to a dose up to 200 cGy with a rapidly delivered 3-ion beam ^{1}H (1000 MeV, 0.24 keV/μm, 60%), ^{16}O (250 MeV/n, 25 keV/μm, 20%) and ^{28}Si (263 MeV/n, 78 keV/μm, 20%) (Raber 2019) or 6- ion beam ^{1}H (1000 MeV, 0.24 keV/μm, 50%), ^{4}He (250 MeV/n, 1.6 keV/μm, 20%), ^{16}O (250 MeV/n, 25 keV/μm, 7.5%), ^{28}Si (263 MeV/n, 78 keV/μm, 7.5%), ^{48}Ti (1000 MeV/n, 107 keV/μm, 7.5%) and ^{56}Fe (1000 MeV/n, 151 keV/μm, 7.5%) (Raber 2020). Detrimental effects that differed between males and females and depended on the cognitive task were observed. Of note, a systematically impaired object recognition for doses of 50 cGy and higher and for both 3-ion and 6-ion beams was also observed, which was consistent with previous single-ion beam studies. For contextual or cued fear memory, no statistically significant irradiation effects were observed, while other studies reported that impairment could be observed depending on the ion type. In addition, several differences between 3-ion and 6-ion beams were noted, including effects on body weight, home cage activity, open field activity/anxiety or depressive-like behavior.

Using the simplified GCRsim beam, Krukowski (2021) showed a detrimental effect to spatial learning for a 50 cGy exposure for male C57B16/J wild-type mice, but not for 100 cGy and not for female mice. This impairment was associated with an inflammatory response characterized by enhanced microglia activation and synaptic alterations in the hippocampus and could be mitigated by inducing a temporary microglia depletion followed by repopulation, which was also observed for ^{4}He irradiation (Krukowski 2018b). Microglia are macrophage cells acting as the main immune response of the CNS and can affect neuronal structure and function, thereby altering cognitive tasks (Krukowski 2021). Contrary to previous single-ion studies, deficits in other behavioral (anxiety, sociability) or cognitive (social memory and recognition memory) tasks were not observed. Considering chronic exposure of mice (BALB/c female and C3H male) to a mixed field of neutrons and photons with a ^{252}Cf emitter, two studies showed different dose-response relationships depending on the measured endpoint, with anticipation of worse performances during space mission for some tasks, and enhanced performances for others (Perez 2020; Holden 2021). CH3 male mice were also exposed to acute or fractionated GCRsim and showed that the effect of time of exposure depended on the behavioral or cognitive tasks as well (Holden 2021).

A recent modeling exercise on the LET dependency of induced deficits in novel object recognition performance revealed that the best fit for the data was a combination of non-targeted effects as well as targeted effects (Shuryak 2021). Although the nature of the non-targeted effects is currently not known, these appear to be an important determinant of CNS functionality in some instances.

3.3.5. Lifespan studies with neutron vs. HZE ions

Weil (2021) investigated the effect of acute vs. chronic exposure to neutrons and acute vs. fractionated exposure to GCRsim on lifespan in BALB/c female and C3H male mice, and histopathology investigation is ongoing. The chronic neutron source was ^{252}Cf with a dose rate of 1 mGy/day and contained 20% of γ-ray contamination (Borak et al., 2019). The mean LET was ~70 keV/μm. The acute exposure was performed at the Radiological Research Accelerator Facility at Columbia University, by bombarding a beryllium target with mixed hydrogen and deuterium beam. The dose rate was 1.2 Gy/hr with γ-ray contamination of ~17%. BALB/c female mice showed a significant decrease of survival that was dose dependent (7 to 10% median life span) for chronic exposure. A 400 mGy low dose rate exposure was less effective than a

400 mGy acute exposure for life shortening. The decrease was not observed for C3H males irradiated with chronic neutrons, but life shortening was observed for acute exposure at 400 mGy. Acute vs. fractionated (19 fractions over 4 weeks) exposures using the GCRsim beam were also evaluated. A decrease in survival of CH3 male mice compared to sham irradiated controls was observed, but no difference was detected between chronic vs. acute exposure. GCR exposure increased life shortening compared to chronic neutron exposure but was less effective than acute neutron exposure (Weil 2021).

4. Workshop discussion

The workshop discussion aimed at determining, based on the existing body of evidence, if the GCRsim as currently defined, adequately represents the radiation environment that will be encountered by humans in deep space behind shielding (ion types and energies) for the multiple endpoints tested and given the practical limitations of any ground-based facility. Where there was evidence suggesting that the GCRsim definition needed improvement, participants also discussed what types of studies should be designed to make these advancements. This section is organized into three parts summarizing the topics discussed at the workshop: (1) areas of consensus, (2) contradictory evidence and (3) questions that have not been addressed yet and will need to be considered for future studies. In some cases, broad topics such as beam ordering may appear in more than one subsection, which reflects the complex nature of the problem being addressed wherein consensus may have been reached on parts of a broad topic, while it was recognized that open questions remain in other parts.

4.1. Areas of consensus

4.1.1. Beam composition

The current GCRsim includes a broad distribution of proton and helium beam energies (Table 1), allowing both dose- and fluence-based quantities from the reference field to be well represented (Simonsen 2020). The HZE component, on the other hand, comprises five discrete beams covering an LET range of 8 keV/μm – 175 keV/μm. A question naturally arises regarding the adequacy of five beams to represent such a broad LET range in a mixture dominated by protons and helium ions (91% of dose, see Table 1). In that regard, workshop participants have compared various endpoints obtained for different beam compositions. Given the same beam order (i.e., proton vs. HZE being delivered first), workshop participants reported no measurable change in sensitivity towards the HZE component for in vitro chromosome aberrations comparing 4-ion and 6-ion beams. Although results for more endpoints and experimental systems are required to draw a firm conclusion, participants agreed that based on current evidence the level of complexity appears to be sufficient for the GCRsim beam as currently defined.

4.1.2. Neutrons

There was an overall agreement that the simulator as currently configured is missing a portion of neutron exposure that would be present in the space environment. Details of the modeling approach used to calculate the GCRsim reference field must be understood to set appropriate context for this discussion (Slaba 2016; Simonsen 2020). The GCRsim reference environment describes the radiation field found within humans behind shielding while in space, encompassing both primary GCR ions as well as the secondary particles produced in shielding and tissue, such as neutrons. Also included in the reference field are a majority of the neutron interaction byproducts that are typically thought of as neutron dose – recoil protons and inelastic reaction products with $Z \leq 2$. Since the corresponding GCRsim proton and helium beams are normalized directly to the reference field fluences, a majority of the neutron dose is accounted for in the GCRsim beam.

Given this context, there are two remaining aspects of the neutron exposure that are missing in the GCRsim. First, when energetic neutrons collide with nuclei in the human body, target fragments with $Z > 2$ can be produced with average energies below ~10 MeV/n. These heavy target fragments deposit energy within μm of their production site, and have LETs exceeding 175 keV/μm. These target fragments are not included in the GCRsim reference field or HZE beam definitions. The contribution of these particles to total dose is small but could have a moderate (on the order of 10%) contribution to cancer risk related quantities (Simonsen 2020). The contribution of these particles to other health risks in space is largely unknown at this time. Second, the spatial correlation and distribution of neutron reaction products are not retained in the GCRsim. Neutron interactions are seemingly randomly distributed throughout the body in space, but at each interaction site, the energy deposited can be quite large due to the multiplicity of charged target fragments produced. These high LET events yield correlated ion tracks traversing a small volume instantaneously and are not retained in the GCRsim sequential beam delivery protocol. Solutions were suggested to overcome these issues.

It was suggested to perform ion irradiation at NSRL and then ship mice to another facility for additional neutron exposure. However, given that the missing neutron component only accounts for roughly 10% of the dose equivalent, decisions to include this neutron component should be a trade-off between the cost and complexity it presents and the improvement in accuracy or additional uncertainty that it provides. Another solution would be to use a hybrid GCRsim method (Fig. 1C), which incorporates shielding in the beam line to produce neutrons and other secondary particles. The direct advantage of this approach would be to recover the correlation of secondary particles produced by neutron interactions within the body. More research is needed to define an optimal hybrid simulator.

4.1.3. Beam delivery order

Another area of consensus regarding beam definition is that the order of ion delivery can be important for highly simplified (2-ion or 3-ion) mixed beams. The impact of ion order for more complex beams (GCRsim or simplified GCRsim) with a significant low LET component remains unclear. Overall, participants agreed that protons should be delivered first and most frequently, as is the case for both the GCRsim beam and the simplified GCRsim beam. This approach best recapitulates the deep space radiation environment where a constant flux of proton and helium ions dominate the field, with periodic HZE ions. Interleaving HZE ions should be maintained for future experiments, unless specifically required otherwise for hypothesis testing.

As detailed in Section 3, several workshop participants reported that switching delivery order for heavy ions vs. protons showed sensitivity for both chromosome aberrations (2-ion beam) in fibroblasts and lung carcinogenesis (3-ion beam). Delivering protons first increased the sensitivity for both endpoints. Previous studies show the importance of beam order with results consistent with data described during this workshop. (Bennett 2007) irradiated cells with split doses of either protons or HZE particles and measured transformation from normal to an anchorage-independent preneoplastic, nontumorigenic phenotype. A much higher number of transformant cells per surviving cell for H (1 GeV) + HZE (1 GeV/n ^{48}Ti or 1 GeV/n ^{56}Fe) as compared to ^{1}H or HZE alone, even for small doses of ^{1}H (i.e., < 20 cGy followed by 20 cGy of ^{56}Fe ions) was observed.

Considering the same endpoint, (Zhou 2006) also investigated sequential beams ^{1}H (1000 MeV) + HZE (^{48}Ti or ^{56}Fe 1000 MeV/n), with different time intervals between the two irradiations (2.5 min – 48 hrs). In this study, a more than an additive effect was obtained with a critical time window between 2.5 min and 1 h for maximized synergetic effects, while longer times (~3 hrs for ^{56}Fe ions and ~6 hrs for ^{48}Ti ions) yielded additive effects, in agreement with previous reports (Sutherland 2005). When testing ^{1}H or HZE only or reversing the order of delivery (HZE + ^{1}H), additive effects were observed. Analysis of survival showed similarity regardless of the beam composition and/or order, and analysis of the cell cycle showed no major differences following irradiation by ^{1}H

ions regardless of the time point, which excludes a change in either cell cycle or survival as the origin of the effect. Further work by (Hada 2007) evaluated formation of chromosome aberrations in human mammary epithelial cells following sequential beams of protons (1000 MeV) and ^{56}Fe ions (1000 MeV/n) using 2 min, 30 min and 60 min intervals between exposures. At intervals of 2 min and 30 min, the aberration yield was greater than additive, while at 60 min additive effects were observed. The authors suggest that following the initial exposure chromatin unwinding at sites of DNA repair render the cells more susceptible to DNA damage by additional exposures.

However, not all endpoints show sensitivity to beam order for mixed beam experiments. One study investigated mixed beam responses for in vitro cell transformation from a preneoplastic to a neoplastic, tumorigenic phenotype (Elmore 2011). Adaptive response has been observed for such an endpoint for both ^{1}H (1000 MeV; $<$ 10 cGy) and ^{56}Fe (1000 MeV/n; $\leq$ 1 cGy), where a small irradiation dose reduced the frequency of neoplastic transformation as compared to the zero-dose baseline, resulting in J-shaped dose-response curves. Whether a small dose of irradiation (10 cGy of ^{1}H or ^{56}Fe) followed by a higher dose (1 Gy of ^{1}H or ^{56}Fe) would induce a protective effect was also evaluated using either 5 min – 15 min (immediate) or 16 h–24 h (delayed) time intervals. Regardless of the testing configuration, an adaptive response was not observed, with a possible exception for 10 cGy ^{56}Fe irradiation followed by 1 Gy ^{1}H irradiation, although the authors pointed out that both the original dose (10 cGy) and time interval might have been too large to observe such outcomes. In any case, responses were no more than additive, indicating no beam order effect for this endpoint.

Another study investigated the effect of sequential irradiation with ^{1}H (50 MeV or 1000 MeV; 1.25 keV/μm or 0.2 keV/μm) followed, at different time points (6 hrs, 24 hrs or 72 hrs), by ^{56}Fe (1000 MeV/n; 151 keV/μm) on micronucleus formation in normal human fibroblasts (Buonanno 2015). Compared to ^{56}Fe ion only irradiation, a reduced number of micronuclei were observed, a mitigating effect that was transient. In addition, unirradiated cells that were co-cultured with cells exposed to the first proton dose were also afforded protection against damage from a subsequent ^{56}Fe exposure.

While the order of the beam (^{1}H vs. HZE) for simplified, 2-ion to 3-ion beams, shows an effect for many endpoints, it remains unclear whether this dependence is still observed for more complex (GCRsim or simplified GCRsim) beams with a dose that is largely dominated by low LET proton and helium components. These 2-ion to 3-ion beam experiments have a higher HZE component than is expected for a realistic intravehicular GCR environment, which could exacerbate the dependence on the ion order and needs to be understood mechanistically.

4.1.4. GCRsim beam standardization

Early ground-based experiments focused on space radiation were heavily influenced by facility constraints wherein only a single particle type or energy could be provided. The notion of switching the beam ion or energy during an experiment is still a relatively new concept, and the remarkable fast switching capability at NSRL is fundamental to the current GCRsim. These technological advancements have given researchers more degrees of freedom in experimental design, particularly in the areas of beam selection and delivery protocols. This increased freedom also introduces challenges when one attempts to synthesize the data from these diverse experimental designs, as is needed to develop consensus models (Shuryak 2022) for radiation quality or dose rate effects used in risk assessment (Simonsen 2021). Investigation of mixed-field effects amplifies this problem as the number of conceivable beam mixtures becomes infinite. Recognizing the potential for such a problem, NASA chose to standardize the GCRsim and simplified GCRsim beams as defined in Tables 1 and 2, respectively. The practical value of beam standardization for such a complex tool as the GCRsim is obvious from the standpoint of data synthesis, cross validation, and long-term research vision. At the same time, it is recognized that over-prescribing experimental parameters can cripple innovation, constrain hypothesis driven research, and hinder necessary breakthroughs. It is within this context that the topic of GCRsim beam standardization was discussed during the workshop.

There was a consensus on the need for GCRsim beam standardization for established biological systems (cells, mice, and rats). Larger animals have been discussed and proposed, such as mini-pigs, and may necessitate adjustments to account for larger tissue shielding and beam modifications. It is important to note however, that the prescription of a standard GCRsim beam would not preclude other mixed fields or single ions to be studied given suitable hypotheses, e.g., for mechanistic understanding or modeling. Indeed, the workshop discussion made it clear that multiple questions pertaining to mixed-field effects remain open and will require the use of unique beam mixtures.

It was generally agreed though that there should be a priority on the use of standardized (GCRsim and simplified GCRsim) beams for early investigations with little or no single beam data to support interrogation of combinatorial effects. As for using the GCRsim or its simplified version, it was suggested that participants with existing datasets and mature research should work with the GCRsim, while newer research could start off with the simplified GCRsim beam. Beam standardization would then facilitate inter-comparability between data across different experiments performed from different institutions and provide space vs. ground reference type of results. It was suggested that beam standardization with the simplified GCRsim may be particularly beneficial for CNS endpoints, where cross-experiment comparisons remain challenging at this time.

4.2. Contradictory results or evidence

4.2.1. Additivity, synergy or antagonism

The current GCRsim design has the advantage of allowing historical datasets based on single ion exposures to support mechanistic understanding and model development for mixed-field effects. A question then arises regarding the combinatorial rules that should be applied to single ion exposures for mixed-field predictions, which is particularly important in the context of risk assessment models (Cucinotta 2013a) where simple additivity is assumed in order to project risk for the ions and energies comprising the complex space environment. The uncertainty associated with this assumption is not accounted for in probabilistic calculations either. Yet, in the presence of non-linearities at low dose associated with non-targeted effects or possible thresholds, simple additivity would likely be invalid. Insights gained from experimental studies and model advancements enable more accurate combinatorial methods to be developed or at least uncertainty to be quantified for the existing simple additivity approach used in the NASA risk model (Simonsen 2021).

Experimental evidence and modeling results obtained so far show diverse results regarding additivity vs. synergy/antagonism for mixed beam exposures (Section 3). In vitro chromosome aberrations data showed synergy or antagonism, which depended on the number of ions included in the beam and on the cell line. Harderian gland data showed either strictly additivity or synergy, and the extent of the effect depended on the dose (Huang 2020). As discussed in Section 4.3.4 it is also important to consider the interplay between the timing of exposures and the complexity of the beam mixture. While issues related to dose-rate were not the focus of this workshop, the impact of time between ions when one considers complex mixed fields like the GCRsim with greater than 30 beams is not yet clear. Additional systematic studies are needed in mature experimental systems to improve clarity.

4.2.2. Experimental protocols standardization

The need for GCRsim beam standardization was discussed in Section 4.1.4 as an area of consensus, with the caveat that alternative beam definitions may be needed to interrogate specific aspects of mixed-field effects. The topic of standardized experimental protocols was also raised. Although no consensus was reached on the issue, the workshop

attendees provided diverse and sometimes contradictory points of view that collectively set important context for future research planning and objectives.

It was recognized that standardization of experimental protocols beyond beam selection is challenging in the context of limited mechanistic understanding. Furthermore, experimental parameters (model system, assay, timing, etc.) often need to be chosen or perturbed such that measurable signals can be optimized to facilitate hypothesis testing while staying within practical limitations such as cost. However, as mentioned in 4.1.4, decisions on experimental design must be balanced against the need to synthesize knowledge gained from the breadth of experimental data to inform human health risk assessment.

One approach was suggested that imposes a degree of standardization. The idea was to pose specific questions requiring the GCRsim that could be examined in multiple experimental systems. However, it was argued that this strategy would only allow analogies to be drawn from seemingly comparable measurements across different systems. The preferred alternative is to identify a catalog of relevant and high priority mechanisms that appear common across studies and enable predictions to be made. Such an approach has been proposed for different stressors in the framework of adverse outcome pathways, with the example of this framework applied to ionizing radiation for its effects in lung cancer (Chauhan 2021).

Another point of conflict that arises, in terms of standardization, while going from animal models to human models, is the use of larger animals. Some participants contended that having larger animals such as pigs would be a better substitute to scale to humans in lieu of mouse and rat models. However, other participants commented that using such larger animals is not yet feasible with current NSRL capabilities and might not provide more insight than the smaller animal models.

Workshop participants agreed that standardization will be particularly important for medical countermeasure (MCM) validation, although no consensus was reached on the prescription of such standards. It was clarified that for each defined endpoint or health risk of interest, a common baseline measure must be identified with a justifiable linkage to a human health outcome from which MCM efficacy can be gauged. Workshop participants concluded that for early stage MCM development or screening, standard assays may not be needed and the use of low-LET sources and methods that allow for high throughput evaluation may be sufficient to establish efficacy and the need for further testing. Later stages of MCM evaluation would necessitate testing with GCRsim using standard measures and predefined model systems.

4.3. Open questions

4.3.1. HZE ion order in the GCRsim

As discussed previously, participants agreed that beam order can influence results for simplified, 2-ion to 3-ion beams, but it is unclear if this dependence is retained within more complex irradiation fields dominated by low LET ions, such as the GCRsim. This sensitivity might also strongly depend on the total dose and dose rate definitions, as was seen for the mixed-field lung carcinogenesis experiments (see Section 3.3.2). Acute exposures showed sensitivity to ion beam order with 3 beam mixtures, but the sensitivity was reduced when the time between individual beams was increased.

In that regard, an experiment to specifically address the question of HZE ion ordering in the GCRsim was in progress and discussed at the workshop. Mice were exposed to the GCRsim beam with all heavy ions delivered at the end of an acute exposure. Results are expected for lung tumor invasiveness at 1-year post-irradiation which may provide more clarity when compared to results for the standard GCRsim ordering. Additional limited experimental cases could be tested, e.g., by testing the sensitivity of the beam delivery order for increasing beam complexity. Knowledge of the underlying mechanisms (Section 3.3.2) is also critical for determining if such effects are relevant for deep space exposure and to ensure adequate ground-based GCR simulations.

4.3.2. Sequential beams as a surrogate for mixed fields

One limitation of the reference field is that the spatial-temporal correlation of the secondary particle shower generated when GCR ions traverse shielding, and tissue is partly lacking. When a heavy ion from the natural GCR environment suffers a nuclear collision within vehicle shielding or tissue, many secondary particles are produced including fragments from the original ion (projectile-like) and fragments from the target (target-like). Projectile-like fragments are produced with an energy and direction very near that of the original ion, while target-like fragments include both energetic, forward directed components and low energy, isotropic components. The possibility exists for multiple projectile-like fragments to traverse the same small volume almost simultaneously, thereby creating a spatial-temporal correlation. Although the current GCRsim beam includes the relevant charged particle secondaries, the aforementioned correlations are lost within the sequential beam protocol.

From a CNS perspective, the timing of ion tracks may be particularly important as these health effects likely involve several regions of the brain rather than just one. Representing the cascade of correlated primary and secondary particle tracks by sequential ion irradiation is an approximation, and it is difficult to test whether it is acceptable. A possibility would be to use a hybrid approach to (at least partly) recover the correlations associated with a secondary ion shower. Monte Carlo simulations of particle traversals for different regions of the brain that quantify such correlations would help clarify if this could be significant.

4.3.3. Low energy HZE ions in the GCRsim

The GCRsim HZE beam energies were chosen, in part, to avoid rapid dose gradients within commonly used experimental systems such as cells, mice, and rats. Low energy HZE beams have the potential to range-out, or come to rest, in some experimental systems, which would yield an internal Bragg peak with significant dose variation in localized regions that may unpredictably influence biological outcomes. Despite the obvious practical rationale for avoiding locally high dose gradients, there are low energy HZE ions in space that will stop within the human body on an individual track basis.

The question was raised regarding the importance of these low energy HZE ions and the value of including them in the GCRsim. For CNS endpoints, the spatial deposition of inhomogeneous doses due to low energy tracks could injure neuronal networks and thus alter several functions involved in multiple regions of the brain. From a physics standpoint, it is very plausible that multiple HZE ions could come to rest in regions of the brain within relevant time scales, which would occur in the context of many more traversals by hydrogen ions, helium ions and highly energetic HZE ions. Monte Carlo simulations should be pursued to better quantify the impact of low-energy particles relative to the bulk of the environment represented by energetic tracks.

4.3.4. Decoupling dose-rate and mixed-field effects

The question of dose rate was voluntarily left out of the discussion, as the purpose of the workshop was to answer questions regarding the adequacy of the mixed-field aspects of the beam, and thus primarily the beam composition (ions, energies, etc.). However, fractionation and dose rate aspects remain as one of the dominant uncertainties in assessing space radiation induced health effects and as discussed, may also affect the questions related to adequacy of the beam composition. The subsequent open question is whether the issues of beam composition and dose rate can be treated separately. Experimental data to assess the dependence of dose rate and chronic vs. acute exposure are forthcoming for high-LET (Sections 3.2.2 and 3.3.2) and neutrons (Section 3.3.5). While dose rate is undoubtably a strong variable, it remains unclear how this affects dose-responses, for instance in vivo results suggest higher carcinogenesis (Section 3.2.2) while in vitro results suggested otherwise (Section 3.3.2). Participants suggested that, just as there is a reference beam field, there should be a reference dose rate.

5. Conclusion

Understanding the biological outcomes associated with exposure to the complex radiation environment in space is a tremendous challenge, but an essential step in the process to achieve safe and productive human space exploration, and to preserve long-term quality of life for space explorers. The GCR simulator at the NASA Space Radiation Laboratory provides an accelerator-based exposure regimen consisting of rapidly switchable ions and energies that approximates the primary and secondary GCR field experienced by the human body within a spacecraft. The GCR simulator is an added capability at NSRL supporting space radiobiology research. As part of a comprehensive research program, the GCRsim will improve risk model predictions, enhance biomarker discovery and validation, and aid countermeasure selection and validation across all major space radiation health risk areas. This information is needed to realize NASA exploration goals. The GCRsim workshop summarized in this report provided an opportunity to evaluate progress of the NASA GCR simulator design and early implementation with a focus on review of the mixed-field composition, order of ion delivery, and early data from computational modeling and biological experimentation. Modeling approaches, experimental constraints, areas of consensus, and questions of concern were also discussed in detail.

The early experimental campaigns were successful with the automated delivery of 33-ion sequential GCRsim reference field taking approximately 75 min with no major interruptions or delays. There were several main lessons learned from this early work related to the complexity of the beam, the order of delivery and evidence for combinatorial effects. The complexity of the GCRsim beam, as currently specified, was considered adequate to represent the radiation environment encountered by humans in deep space behind shielding. However further work is required to fully address this issue with specific studies focused on comparing data acquired using the 33-ion GCRsim reference field to less complex mixtures including the simplified 5-ion GCRsim. Two additional caveats were also discussed. One is the lack of low energy HZE ions, omitted to avoid exposure "hot spots" in experimental models, but that is present in the spaceflight environment. The other caveat is the lack of a small fraction of neutron exposure and related spatial-temporal correlation of ion tracks occurring in space. These issues may be addressed by considering a hybrid method at the NSRL beamline, but development and implementation will require further research.

The order of ion delivery appears to be appropriate. Early experimental data suggests ion order may be less important for a complex radiation field, such as the GCRsim, which spans a broad range of LET. Experimental results from simple mixed-field exposures, on the other hand, seem to be more sensitive to ion order and timing protocols. Careful design of experimental studies directed at bounding this issue are important to pursue and will provide necessary validation of this strategy. There was varied evidence for combinatorial effects (additivity/synergy/antagonism), and general agreement that further data is required to determine how generalizable these concepts may be across the main human health risk areas. There was also overall agreement that the standardized GCRsim or simplified 5-ion GCRsim beams should be preferred for experimental studies that are not directly addressing hypothesis driven questions related to order of ion delivery, validation of combinatorial effects or when single ion studies are not clearly justified, which will facilitate comparison of experimental results across different studies and risk areas. The issue of standardization was also discussed with regards to experimental models and protocols, and it was recognized that standardization beyond beam selection would be challenging given the current incomplete mechanistic understanding of the complex outcomes of space radiation exposure but would be important to consider for future biomarker and/or medical countermeasure studies. While outside the scope of this workshop, open questions remain regarding the use of rapidly delivered sequential beams as a surrogate for chronic exposures in the space environment, the importance of which may vary depending on the endpoints and timescales of biological processes under evaluation.

In summary, the overarching conclusion of the workshop discussions was that the current GCRsim reference field and delivery approach are scientifically sound and state of the art. This capability provides a step forward, enabling space radiobiology studies focused on addressing key issues for protection of humans during space travel.

Funding

This work was supported by the Human Research Program of the Space Operations Mission Directorate of the National Aeronautics and Space Administration (NASA) [JLH, TCS, RBN, LCS] and by the Human Health and Performance contract NNJ15HK11B [ZSP]; the NASA Langley Cooperative Agreement 80LARC17C0004 [NK FP, SR]; NASA grants 80JSC02IT0017, NNJ16HP22I and supported by the U.S. Department of Energy Office of Science under Contract No. DE-AC02–05CH11231 [EAB]; NASA grants NNX14AE73G, NNX15AI22G, NNX16AC40G [RAB]; NNX15AI21G [AJF]; NNJ16HP231 [AK]; NNX16AR97G [MH]: NNX15AK13G [MMW]; NNX16AE08G, NNX15AI21G [JWS, distinguished Southland Financial Corporation chair in Geriatrics Research] and the Harold Simmons NCI Designated Comprehensive Cancer Center Support Grant CA142543 [JWS].

Statement on the use of animals

The animal facility at BNL follows the “Guide for the Care and Use of Laboratory Animals”, enforced by the Office of Laboratory Animal Welfare (OLAW Animal Welfare Assurance Number D16–00067). The facility has been accredited by the Association for the Assessment and Accreditation of Laboratory Animal Care since 1966, and all research involving animals must comply with the Public Health Service “Policy on Humane Care and Use of Laboratory Animals.” All research described in this document was reviewed and approved by the BNL Institutional Animal Care and Use Committee prior to initiation.

Declaration of Competing Interest

The authors declare that they have no known competing financial interests or personal relationships that could have appeared to influence the work reported in this paper. All authors declare that they have no conflicts of interest related to funding, personal gain, or financial interest. Although several authors work directly [JLH, SRB, RBN, LCS] as employees or indirectly as contractors [NK, ZSP, FP, SR] for NASA, the views and opinions expressed herein are those of the authors and do not necessarily reflect the views of NASA or the United States government and do not imply NASA supported program direction.

Acknowledgements

The authors are grateful to Dr. Walter Schimmerling for guiding and organizing efforts throughout the development and implementation of the NSRL GCRsim and for his significant contributions to the various workshops and organized technical interchanges summarized herein. The authors are also grateful to Dr. Rainer Sachs for thoughtful questions and discussions over the past several years. His inputs contributed greatly to identifying important open questions discussed at the workshop and in this report. We also would like to acknowledge the NSRL staff for their efforts in making the GCRsim a practical reality for space radiation research.

References

Acharya, M.M., Baulch, J.E., Klein, P.M., Baddour, A.A.D., Apodaca, L.A., Kramár, E.A., Alikhani, L., Garcia Jr, C., Angulo, M.C., Batra, R.S., Fallgren, C.M., 2019. New concerns for neurocognitive function during deep space exposures to chronic, low

dose-rate, neutron radiation. eNeuro 6 (4). https://doi.org/10.1523/ENEURO.0094-19.2019.
Agostinelli, S., et al., 2003. Geant4—a simulation toolkit. Nucl. Instrum. Methods Phys. Res. A 506, 250–303. https://doi.org/10.1016/S0168-9002(03)01368-8.
Alpen, E.L., Powers-Risius, P., Curtis, S.B., DeGuzman, R., 1993. Tumorigenic potential of high-Z, high-LET charged-particle radiations. Radiat. Res. 136 (3), 382–391. https://doi.org/10.2307/3578551.
Alpen, E.L., Powers-Risius, P., Curtis, S.B., DeGuzman, R., Fry, R.J.M., 1994. Fluence-based relative biological effectiveness for charged particle carcinogenesis in mouse harderian gland. Adv. Space Res. 14 (10), 573–581. https://doi.org/10.1016/0273-1177(94)90512-6.
Asselin-Labat, M.-L., Rampersad, R., Xu, X., Ritchie, M.E., Michalski, J., Huang, L., Onaitis, M.W., 2017. High-LET radiation increases tumor progression in a K-Ras-driven model of lung adenocarcinoma. Radiat. Res. 188 (5), 642–650. https://doi.org/10.1667/RR14794.1.
Azasi, Y., Gallagher, S.K., Diouf, A., Dabbs, R.A., Jin, J., Mian, S.Y., Narum C. A. Long, D. L., Gaur, D., Draper, S.J., Fay, M.P., 2020. Bliss' and Loewe's additive and synergistic effects in Plasmodium falciparum growth inhibition by AMA1-RON2L, RH5, RIPR and CyRPA antibody combinations. Sci. Rep. 10 (1), 1–12. https://doi.org/10.1038/s41598-020-67877-8.
Bennett, P.V., Cutter, N.C., Sutherland, B.M., 2007. Split-dose exposures versus dual ion exposure in human cell neoplastic transformation. Radiat. Environ. Biophys. 46 (2), 119–123. https://doi.org/10.1007/s00411-006-0091-y.
Blakely, E., Bakke, J., Grover, A., Rusek, A., Snyder, D., Rhone, J., Parra, M., Bjornstad, K., Mao, J., Hada, M., Sachs, R., Chang, P., 2021. Murine Harderian Gland (HG) tumorigenesis after 3 HZE-mixed field exposures. Presented At the Human Research Program Investigators Workshop. Online, National Aeronautics and Space Administration. February.
Borak, T.B., Heilbronn, L.H., Krumland, N., Weil, M.M., 2019. Design and dosimetry of a facility to study health effects following exposures to fission neutrons at low dose rates for long durations. Int. J. Radiat. Biol. 97 (8), 1063–1076. https://doi.org/10.1080/09553002.2019.1688884.
Britten, R.A., Davis, L.K., Jewell, J.S., Miller, V.D., Hadley, M.M., Sanford, L.D., Machida, M., Lonart, G., 2014. Exposure to mission relevant doses of 1 GeV/nucleon 56Fe particles leads to impairment of attentional set-shifting performance in socially mature rats. Radiat. Res. 182 (3), 292–298. https://doi.org/10.1667/RR3766.1.
Britten, R.A., Duncan, V.D., Fesshaye, A., Rudobeck, E., Nelson, G.A., Vlkolinsky, R., 2020b. Altered cognitive flexibility and synaptic plasticity in the rat prefrontal cortex after exposure to low (≤ 15 cGy) doses of ^{28}Si radiation. Radiat. Res. 193 (3), 223–235. https://doi.org/10.1667/RR15458.1.
Britten, R.A., Fesshaye, A.S., Duncan, V.D., Wellman, L.L., Sanford, L.D., 2020a. Sleep fragmentation exacerbates executive function impairments induced by low doses of Si ions. Radiat. Res. 194 (2), 116–123. https://doi.org/10.1080/09553002.2019.1694190.
Britten, R.A., Jewell, J.S., Duncan, V.D., Hadley, M.M., Macadat, E., Musto, A.E., La Tessa, C., 2018. Impaired attentional set-shifting performance after exposure to 5 cGy of 600 MeV/n ^{28}Si particles. Radiat. Res. 189 (3), 273–282. https://doi.org/10.1667/RR14627.1.
Britten, Richard A., Fesshaye, Arriyam, Ihle, Peter, Wheeler, Andrew, Baulch, Janet E., Limoli, Charles L., Stark, Craig E., 2022. Dissecting differential complex behavioral responses to simulated space radiation exposures. Radiat. Res. 197 (3), 289–297. https://doi.org/10.1667/RADE-21-00068.1. March 1.
Buonanno, M., De Toledo, S.M., Howell, R.W., Azzam, E.I., 2015. Low-dose energetic protons induce adaptive and bystander effects that protect human cells against DNA damage caused by a subsequent exposure to energetic iron ions. J. Radiat. Res. (Tokyo) 56 (3), 502–508. https://doi.org/10.1093/jrr/rrv005.
Burket, J.A., Matar, M., Fesshaye, A., Pickle, J.C., Britten, R.A., 2021. Exposure to low (≤ 10 cGy) doses of ^{4}He particles leads to increased social withdrawal and loss of executive function performance. Radiat. Res. 196 (4), 345–354. https://doi.org/10.1667/RADE-20-00251.1.
Cekanaviciute, E., Rosi, S., Costes, S.V., 2018. Central nervous system responses to simulated galactic cosmic rays. Int. J. Mol. Sci. 19 (11), 3669. https://doi.org/10.3390/ijms19113669.
Chancellor, J.C., Guetersloh, S.B., Blue, R.S., Cengel, K.A., Ford, J.R., Katzgraber, H.G., 2017. Targeted Nuclear Spallation from Moderator Block Design For a Ground-Based Space Radiation Analog. *arXiv preprint arXiv:1706.02727*. http://arxiv.org/abs/1706.02727.
Chang, P.Y., Cucinotta, F.A., Bjornstad, K.A., Bakke, Ja., Rosen, C.J., Du, N., Fairchild, D. G., Cacao, E., Blakely, E.A., 2016. Harderian gland tumorigenesis: low-dose and LET response. Radiat. Res. 185 (5), 449–460. https://doi.org/10.1667/RR14335.1.
Chauhan, V., Sherman, S., Said, Z., Yauk, C.L., Stainforth, R., 2021. A case example of a radiation-relevant adverse outcome pathway to lung cancer. Int. J. Radiat. Biol. 97 (1), 68–84. https://doi.org/10.1080/09553002.2021.1969466.
Cucinotta, F.A., Cacao, E., 2019. Risks of cognitive detriments after low dose heavy ion and proton exposures. Int. J. Radiat. Biol. 95 (7), 985–998. https://doi.org/10.1080/09553002.2019.1623427.
Cucinotta, F.A., Kim, M.H.Y., Chappell, L.J., 2013a. Space Radiation Cancer Risk Projections and Uncertainties-2012. NASA/TP-2013-217375.
Cucinotta, F.A., Kim, M.H.Y., Chappell, L.J., Huff, J.L., 2013b. How safe is safe enough? Radiation risk for a human mission to Mars. PLoS One 8 (10), e74988. https://doi.org/10.1371/journal.pone.0074988.
Cucinotta, F.A., Schimmerling, W., Blakely, E.A., Hei, T.K., 2021. A proposed change to astronaut exposures limits is a giant leap backwards for radiation protection. Life Sci. Space Res. 31, 59–70. https://doi.org/10.1016/j.lssr.2021.07.005.
Davis, C.M., DeCicco-Skinner, K.L., Roma, P.G., Hienz, R.D., 2014. Individual differences in attentional deficits and dopaminergic protein levels following exposure to proton radiation. Radiat. Res. 181 (3), 258–271. https://doi.org/10.1667/RR13359.1.
Durante, M., George, K., Gialanella, G., Grossi, G., La Tessa, C., Manti, L., Miller, J., Pugliese, M., Scampoli, P., Cucinotta, F.A., 2005. Cytogenetic effects of high-energy iron ions: dependence on shielding thickness and material. Radiat. Res. 164 (4), 571–576. https://doi.org/10.1667/RR3362.1.
Elmore, E., Lao, X.Y., Kapadia, R., Swete, M., Redpath, J.L., 2011. Neoplastic transformation in vitro by mixed beams of high-energy iron ions and protons. Radiat. Res. 176 (3), 291–302. https://doi.org/10.1667/rr2646.1.
Fornace, A., Suman, S., Shay, J., Meltzer, P., Brenner, D., 2021. Space radiation-induced tumorigenesis, risk modeling, long-term injury responses, and mitigation strategy: NSCOR project update. Presented At the Human Research Program Investigators Workshop. Online, National Aeronautics and Space Administration. February.
George, K., Cucinotta, F.A., 2007. The influence of shielding on the biological effectiveness of accelerated particles for the induction of chromosome damage. Adv. Space Res. 39 (6), 1076–1081. https://doi.org/10.1016/j.asr.2007.01.004.
George, K., Durante, M., Willingham, V., Wu, H., Yang, T.C., Cucinotta, F.A., 2003b. Biological effectiveness of accelerated particles for the induction of chromosome damage measured in metaphase and interphase human lymphocytes. Radiat. Res. 160 (4), 425–435. https://doi.org/10.1667/RR3064.
George, K., Durante, M., Wu, H., Willingham, V., Cucinotta, F.A., 2003a. In vivo and in vitro measurements of complex-type chromosomal exchanges induced by heavy ions. Adv. Space Res. 31 (6), 1525–1535. https://doi.org/10.1016/s0273-1177(03)00088-7.
George, K.A., Hada, M., Chappell, L., Cucinotta, F.A., 2013. Biological effectiveness of accelerated particles for the induction of chromosome damage: track structure effects. Radiat. Res. 180 (1), 25–33. https://doi.org/10.1667/RR3291.1.
Gordeev, I.S., Timoshenko, G.N., 2021. A new type of ground-based simulator of radiation field inside a spacecraft in deep space. Life Sci. Space Res. 30, 66–71. https://doi.org/10.1016/j.lssr.2021.05.002.
Hada, M., Meader, J.A., Cucinotta, F.A., Gonda, S.R., Wu, H., 2007. Chromosome aberrations induced by dual exposure of protons and iron ions. Radiat. Environ. Biophys. 46 (2), 125–129. https://doi.org/10.1007/s00411-006-0083-y.
Hada, M., Slaba, T.C., Patel, Z., Chang, P., Saganti, P., Plante, I., Blakely, E., Rhone, J., Mao, J.H., Bakke, J., Doppalapudi, R., 2021. Chromosome Aberrations Induced By GCR-simulated Mixed-Beam Exposure in Human and Mouse Cells-Computational Model Prediction and Biological Validation, 43. 43rd COSPAR Scientific Assembly, p. 1854. Held 28 January-4 February.
Hadley, M.M., Davis, L.K., Jewell, J.S., Miller, V.D., Britten, R.A., 2016. Exposure to mission-relevant doses of 1 GeV/n 48Ti particles impairs attentional set-shifting performance in retired breeder rats. Radiat. Res. 185 (1), 13–19. https://doi.org/10.1667/RR14086.1.
Ham, D.W., Song, B., Gao, J., Yu, J., Sachs, R.K., 2017. Synergy theory in radiobiology. Radiat. Res. 189 (3), 225–237. https://doi.org/10.1667/RR14948.1.
Holden, S., Perez, R., Hall, R., Fallgren, C.M., Ponnaiya, B., Garty, G., Brenner, D.J., Weil, M.M., Raber, J., 2021. Effects of acute and chronic exposure to a mixed field of neutrons and photons and single or fractionated simulated galactic cosmic ray exposure on behavioral and cognitive performance in mice. Radiat. Res. 196 (1), 31–39. https://doi.org/10.1667/RADE-20-00228.1.
Huang, E.G., Lin, Y., Ebert, M., Ham, D.W., Zhang, C.Y., Sachs, R.K., 2019. Synergy theory for murine harderian gland tumours after irradiation by mixtures of high-energy ionized atomic nuclei. Radiat. Environ. Biophys. 58 (2), 151–166. https://doi.org/10.1007/s00411-018-00774-x.
Huang, E.G., Wang, R.-Y., Xie, L., Chang, P., Yao, G., Zhang, B., Ham, D.W., Lin, Y., Blakely, E.A., Sachs, R.K., 2020. Simulating galactic cosmic ray effects: synergy modeling of murine tumor prevalence after exposure to two one-ion beams in rapid sequence. Life Sci. Space Res. 25, 107–118. https://doi.org/10.1016/j.lssr.2020.01.001.
Jewell, J.S., Duncan, V.D., Fesshaye, A., Tondin, A., Macadat, E., Britten, R.A., 2018. Exposure to ≤ 15 cGy of 600 MeV/n ^{56}Fe particles impairs rule acquisition but not long-term memory in the attentional set-shifting assay. Radiat. Res. 190 (6), 565–575. https://doi.org/10.1667/RR15085.1.
Kiffer, F., Boerma, M., Allen, A., 2019. Behavioral effects of space radiation: a comprehensive review of animal studies. Life Sci. Space Res. 21, 1–21. https://doi.org/10.1016/j.lssr.2019.02.004.
Kim, M.-H.Y., Rusek, A., Cucinotta, F.A., 2015. Issues for simulation of galactic cosmic ray exposures for radiobiological research at ground-based accelerators. Front. Oncol. 5, 122. https://doi.org/10.3389/fonc.2015.00122.
Kronenberg, A., Gauny, S., Criddle, K., Vannais, D., Ueno, A., Kraemer, S., Waldren, C.A., 1995. Heavy ion mutagenesis: linear energy transfer effects and genetic linkage. Radiat. Environ. Biophys. 34 (2), 73–78. https://doi.org/10.1007/BF01275209.
Kronenberg, A., Little, J.B., 1989. Locus specificity for mutation induction in human cells exposed to accelerated heavy ions. Int. J. Radiat. Biol. 55 (6), 913–924. https://doi.org/10.1080/09553008914550961.
Kronenberg, A., Tabocchini, M., Guida, P., Snijders, A., Celniker, S., 2021. Dose rate effects and GCR simulation in cancer relevant endpoints. Presented At the Human Research Program Investigators Workshop. Online, National Aeronautics and Space Administration. February.
Krukowski, K., Feng, X., Paladini, M.S., Chou, A., Sacramento, K., Grue, K., Riparip, L.-K., Jones, T., Campbell-Beachler, M., Nelson, G., Rosi, S., 2018b. Temporary microglia-depletion after cosmic radiation modifies phagocytic activity and prevents cognitive deficits. Sci. Rep. 8 (1), 1–13. https://doi.org/10.1038/s41598-018-26039-7.
Krukowski, K., Grue, K., Becker, M., Elizarraras, E., Frias, E.S., Halvorsen, A., Koenig-Zanoff, M., Frattini, V., Nimmagadda, H., Feng, X., Jones, T., 2021. The impact of deep space radiation on cognitive performance: from biological sex to biomarkers to

countermeasures. Sci. Adv. 7 (42), eabg6702. https://doi.org/10.1038/s41598-018-26039-7.
Krukowski, K., Grue, K., Frias, E.S., Pietrykowski, J., Jones, T., Nelson, G., Rosi, S., 2018a. Female mice are protected from space radiation-induced maladaptive responses. Brain Behav. Immun. 74, 106–120. https://doi.org/10.1016/j.bbi.2018.08.008.
Kumar, S., Suman, S., Vs Kallakury, B., Moon, B.-H., Fornace, A.J., Datta, K., 2019. Inverse effect of ^{28}Si and ^{56}Fe radiation on intestinal tumorigenesis vs. carcinogenesis in APC$^{1638N/+}$ mice. In: Proceedings of the American Association for Cancer Research Annual Meeting 2019; 2019 Mar 29-Apr 3, 79. AACR; Cancer Res, Atlanta, GA. Philadelphia (PA), p. 3728. https://doi.org/10.1158/1538-7445.AM2019-3728. Abstract no.
Lederer, S., Dijkstra, T.M., Heskes, T., 2019. Additive dose response models: defining synergy. Front. Pharmacol. 10, 1384. https://doi.org/10.3389/fphar.2019.01384.
Little, M.P., Hoel, D.G., Molitor, J., Boice Jr, J.D., Wakeford, R., Muirhead, C.R., 2008. New models for evaluation of radiation-induced lifetime cancer risk and its uncertainty employed in the UNSCEAR 2006 report. Radiat. Res. 169 (6), 660–676. https://doi.org/10.1667/RR1091.1.
Liu, B., Hinshaw, R.G., Le, K.X., Park, M.A., Wang, S., Belanger, A.P., Dubey, S., Frost, J. L., Shi, Q., Holton, P., Trojanczyk, L., 2019. Space-like ^{56}Fe irradiation manifests mild, early sex-specific behavioral and neuropathological changes in wildtype and Alzheimer's-like transgenic mice. Sci. Rep. 9 (1), 1–17. https://doi.org/10.1038/s41598-019-48615-1.
Loewe, S., 1928. Die quantitativen probleme der pharmakologie. Ergebnisse Physiol. 27 (1), 47–187. https://doi.org/10.1007/BF02322290.
Loewe, S., Muischnek, H., 1926. Ueber kombinationswirkungen. I. Mitteilung hilfsmittel der fragestellung. Arch. Exp. Pathol. Pharmakol. 114, 313–326. https://doi.org/10.1007/BF01952257.
Luitel, K., Bozeman, R., Kaisani, A., Kim, S.B., Barron, S., Richardson, J.A., Shay, J.W., 2018. Proton radiation-induced cancer progression. Life Sci. Space Res. 19, 31–42. https://doi.org/10.1016/j.lssr.2018.08.002.
Luitel, K., Kim, S.B., Barron, S., Richardson, J.A., Shay, J.W., 2020. Lung cancer progression using fast switching multiple ion beam radiation and countermeasure prevention. Life Sci. Space Res. 24, 108–115. https://doi.org/10.1016/j.lssr.2019.07.011.
NCRP, National Council on Radiation Protection and Measurements, 2019. Radiation Exposure in Space and the Potential For Central Nervous System Effects: Phase II, 183. National Council on Radiation Protection and Measurement, Bethesda. *NCRP Report*.
Norbury, J.W., Schimmerling, W., Slaba, T.C., Azzam, E.I., Badavi, F.F., Baiocco, G., Benton, E., Bindi, V., Blakely, E.A., Blattnig, S.R., Boothman, D.A., Borak, T.B., Britten, R.A., Curtis, S., Dingfelder, M., Durante, M., Dynan, W.S., Eisch, A.J., Elgart, T.S., Goodhead, D.T., Guida, P.M., Heilbronn, L.H., Hellweg, C.E., Huff, J.L., Kronenberg, A., La Tessa, C., Lowenstein, D.I., Miller, J., Morita, T., Narici, L., Nelson, G.A., Norman, R.B., Ottolenghi, A., Patel, Z.S., Reitz, G., Rusek, A., Schreurs, A.S., Scott-Carnell, L.A., Semones, E., Shay, J.W., Shurshakov, V.A., Sihver, L., Simonsen, L.C., Story, M.D., Turker, M.S., Uchihori, Y., Williams, J., Zeitlin, C.J, 2016. Galactic cosmic ray simulation at the NASA Space Radiation Laboratory. Life Sci. Space Res. 8, 38–51. https://doi.org/10.1016/j.lssr.2016.02.001.
NRC, National Research Council, 2006. Health Risks from Exposure to Low Levels of Ionizing Radiation. BEIR VII Phase 2 Report. National Academies Press.
Parihar, V.K., Allen, B., Tran, K.K., Macaraeg, T.G., Chu, E.M., Kwok, S.F., Chmielewski, N.N., Craver, B.M., Baulch, J.E., Acharya, M.M., Cucinotta, F.A., 2015. What happens to your brain on the way to Mars. Sci. Adv. 1 (4), e1400256 https://doi.org/10.1126/sciadv.1400256.
Parihar, V.K., Allen, B.D., Caressi, C., Kwok, S., Chu, E., Tran, K.K., Chmielewski, N.N., Giedzinski, E., Acharya, M.M., Britten, R.A., Baulch, J.E., 2016. Cosmic radiation exposure and persistent cognitive dysfunction. Sci. Rep. 6 (1), 1–14. https://doi.org/10.1038/srep34774.
Parihar, V.K., Maroso, M., Syage, A., Allen, B.D., Angulo, M.C., Soltesz, I., Limoli, C.L., 2018. Persistent nature of alterations in cognition and neuronal circuit excitability after exposure to simulated cosmic radiation in mice. Exp. Neurol. 305, 44–55. https://doi.org/10.1016/j.expneurol.2018.03.009.
Perez, R.E., Younger, S., Bertheau, E., Fallgren, C.M., Weil, M.M., Raber, J., 2020. Effects of chronic exposure to a mixed field of neutrons and photons on behavioral and cognitive performance in mice. Behav. Brain Res. 379, 112377 https://doi.org/10.1016/j.bbr.2019.112377.
Plante, I., Ponomarev, A., Patel, Z., Slaba, T.C., Hada, M., 2019a. RITCARD: radiation-induced tracks, chromosome aberrations, repair and damage. Radiat. Res. 192 (3), 282–298. https://doi.org/10.1667/RR15250.1.
Plante, I., Slaba, T.C., Shavers, Z., Hada, M., 2019b. A bi-exponential repair algorithm for radiation-induced double-strand breaks: application to simulation of chromosome aberrations. Genes 10 (11), 936. https://doi.org/10.3390/genes10110936.
Preston, D.L., Ron, E., Tokuoka, S., Funamoto, S., Nishi, N., Soda, M., Mabuchi, K., Kodama, K., 2007. Solid cancer incidence in atomic bomb survivors: 1958–1998. Radiat. Res. 168 (1), 1–64. https://doi.org/10.1667/RR0763.1.
Raber, J., Allen, A.R., Sharma, S., Allen, B., Rosi, S., Olsen, R.H., Davis, M.J., Eiwaz, M., Fike, J.R., Nelson, G.A., 2016. Effects of proton and combined proton and ^{56}Fe radiation on the hippocampus. Radiat. Res. 185 (1), 20–30. https://doi.org/10.1667/RR14222.1.
Raber, J., Fuentes Anaya, A., Torres, E.R.S., Lee, J., Boutros, S., Grygoryev, D., Hammer, A., Kasschau, K.D., Sharpton, T.J., Turker, M.S., Kronenberg, A., 2020. Effects of six sequential charged particle beams on behavioral and cognitive performance in B6D2F1 female and male mice. Front. Physiol. 11, 959. https://doi.org/10.3389/fphys.2020.00959.
Raber, J., Holden, S., Sudhakar, R., Hall, R., Glaeser, B., Lenarczyk, M., Rockwell, K., Nawarawong, N., Sterrett, J., Perez, R., Leonard, S.W., 2021. Effects of 5-ion beam irradiation and hindlimb unloading on metabolic pathways in plasma and brain of behaviorally tested WAG/Rij rats. Front. Physiol. 12 https://doi.org/10.3389/fphys.2021.746509.
Raber, J., Yamazaki, J., Torres, E.R.S., Kirchoff, N., Stagaman, K., Sharpton, T., Turker, M.S., Kronenberg, A., 2019. Combined effects of three high-energy charged particle beams important for space flight on brain, behavioral and cognitive endpoints in B6D2F1 female and male mice. Front. Physiol. 10, 179. https://doi.org/10.3389/fphys.2019.00179.
Schaeffer, E.A., Blackwell, A.A., Oltmanns, J.O., Einhaus, R., Lake, R., Piwowar Hein, C., Baulch, J.E., Limoli, C.L., Ton, S.T., Kartje, G.L., Wallace, D.G., 2022. Differential organization of open field behavior in mice following acute or chronic simulated GCR exposure. Behav. Brain Res. 416, 113577 https://doi.org/10.1016/j.bbr.2021.113577.
Schuy, C., Weber, U., Durante, M., 2020. Hybrid active-passive space radiation simulation concept for GSI and the future FAIR facility. Front. Phys. 337. https://doi.org/10.3389/fphy.2020.00337.
Shuryak, I., Brenner, D.J., Blattnig, S.R., Shukitt-Hale, B., Rabin, B.M., 2021. Modeling space radiation induced cognitive dysfunction using targeted and non-targeted effects. Sci. Rep. 11 (1), 1–8. https://doi.org/10.1038/s41598-021-88486-z.
Shuryak, I., Fornace Jr, A.J., Datta, K., Suman, S., Kumar, S., Sachs, R.K., Brenner, D.J., 2017. Scaling human cancer risks from low LET to high LET when dose-effect relationships are complex. Radiat. Res. 187 (4), 486–492. https://doi.org/10.1667/RR009CC.1.
Shuryak, I., Slaba, T.C., Plante, I., Poignant, F., Blattnig, S.R., Brenner, D.J., 2022. A practical approach for continuous in situ characterization of radiation quality factors in space. Sci. Rep. 12 (1), 1–10. https://doi.org/10.1038/s41598-022-04937-1.
Simonsen, L.C., Slaba, T.C., 2021. Improving astronaut cancer risk assessment from space radiation with an ensemble model framework. Life Sci. Space Res. 31, 14–28. https://doi.org/10.1016/j.lssr.2021.07.002.
Simonsen, L.C., Slaba, T.C., Guida, P., Rusek, A., 2020. NASA's first ground-based galactic cosmic ray simulator: enabling a new era in space radiobiology research. PLoS Biol. 18 (5), e3000669 https://doi.org/10.1371/journal.pbio.3000669.
Slaba, T.C., Blattnig, S.R., Norbury, J.W., Rusek, A., La Tessa, C., 2016. Reference field specification and preliminary beam selection strategy for accelerator-based GCR simulation. Life Sci. Space Res. 8, 52–67. https://doi.org/10.1016/j.lssr.2016.01.001.
Slaba, T.C., Blattnig, S.R., Walker, S.A., Norbury, J.W., 2015. A Reference Field for GCR Simulation and an LET-based Implementation at NSRL. at the NASA Human Research Program Investigators Workshop, Galveston, TX. January.
Slaba, T.C., Plante, I., Ponomarev, A., Patel, Z.S., Hada, M., 2020. Determination of chromosome aberrations in human fibroblasts irradiated by mixed fields generated with shielding. Radiat. Res. 194 (3), 246–258. https://doi.org/10.1667/RR15366.1.
Soler, I., Yun, S., Reynolds, R.P., Whoolery, C.W., Tran, F.H., Kumar, P.L., Rong, Y., DeSalle, M.J., Gibson, A.D., Stowe, A.M., Kiffer, F.C., Eisch, A.J., 2021. Multi-domain touchscreen-based cognitive assessment of C57BL/6 J female mice shows whole-body exposure to 56Fe particle space radiation in maturity improves discrimination learning yet impairs stimulus-response rule-based habit learning. Front. Behav. Neurosci. 15, 722780 https://doi.org/10.3389/fnbeh.2021.722780.
Sridharan, D.M., Asaithamby, A., Blattnig, S.R., Costes, S.V., Doetsch, P.W., Dynan, W.S., Hahnfeldt, P., Hlatky, L., Kidane, Y., Kronenberg, A., Naidu, M.D., 2016. Evaluating biomarkers to model cancer risk post cosmic ray exposure. Life Sci. Space Res. 9, 19–47. https://doi.org/10.1016/j.lssr.2016.05.004.
Suman, S., Kumar, S., Moon, B.H., Angdisen, J., Kallakury, B.V., Fornace, A.J., Datta, K., 2019. Heavy-ion space radiation exposure is a potential risk factor for gastrointestinal tumorigenesis even at extremely low doses. Cancer Res. 79, 3729. https://doi.org/10.1016/j.lssr.2020.07.001. -3729.
Sutherland, B.M., Cuomo, N.C., Bennett, P.V., 2005. Induction of anchorage-independent growth in primary human cells exposed to protons or HZE ions separately or in dual exposures. Radiat. Res. 164 (4), 493–496. https://doi.org/10.1667/rr3357.1.
Takahashi, S., Tashiro, M., Hidema, J., Higashitani, A., Adachi, T., Zhang, S., Guirguis, F. N.L., Yoshida, Y., Nagamatsu, A., Hada, M., Takeuchi, K., Takahashi, T., Sekitomi, Y., 2020. Combined environment simulator for low-dose-rate radiation and partial gravity of moon and Mars. Life 10, 274. https://doi.org/10.3390/life10110274.
Timoshenko, G.N., Krylov, A.R., Paraipan, M., Gordeev, I.S., 2017. Particle accelerator-based simulation of the radiation environment on board spacecraft for manned interplanetary missions. Radiat. Meas. 107, 27–32. https://doi.org/10.1016/j.radmeas.2017.10.006.
UNSCEAR, United Nations Scientific Committee on the Effects of Atomic Radiation. "Sources and Effects of Ionizing Radiation. UNSCEAR 2006 Report to the General Assembly, With Scientific Annexes." New York: United Nations, (2008). http://books.google.com/books?id=M_ElAQAAMAAJ.
Valinia, A., Allen, J.R., Francisco, D.R., Minow, J.I., Pellish, J.A., Vera, A.H., 2022. Safe Human Expeditions Beyond Low Earth Orbit (LEO). NASA TM 20220002905, NESC RP 20-01589.
Weil, M., Ullrich, R., Ding, L., Emmett, M., Yu, Y., Udho, E., Bacher, J., Halberg, R., Minnier, J., Raber, J., Story, M., 2021. Carcinogenesis NSCOR: overview. Presented

At the Human Research Program Investigators Workshop. Online, National Aeronautics and Space Administration. February.

Whoolery, C.W., Yun, S., Reynolds, R.P., Lucero, M.J., Soler, I., Tran, F.H., Ito, N., Redfield, R.L., Richardson, D.R., Shih, H.Y., Rivera, P.D., Chen, B.P.C., Birnbaum, S. G., Stowe, A.M., Eisch, A.J., 2019. Multi-domain cognitive assessment of male mice reveals whole body exposure to space radiation is not detrimental to high-level cognition and actually improves pattern separation. Sci. Rep. 10 (1), 2737. https://doi.org/10.1038/s41598-020-59419-z.

Zhou, G., Bennett, P.V., Cutter, N.C., Sutherland, B.M., 2006. Proton-HZE-particle sequential dual-beam exposures increase anchorage-independent growth frequencies in primary human fibroblasts. Radiat. Res. 166 (3), 488–494. https://doi.org/10.1667/RR0596.1.